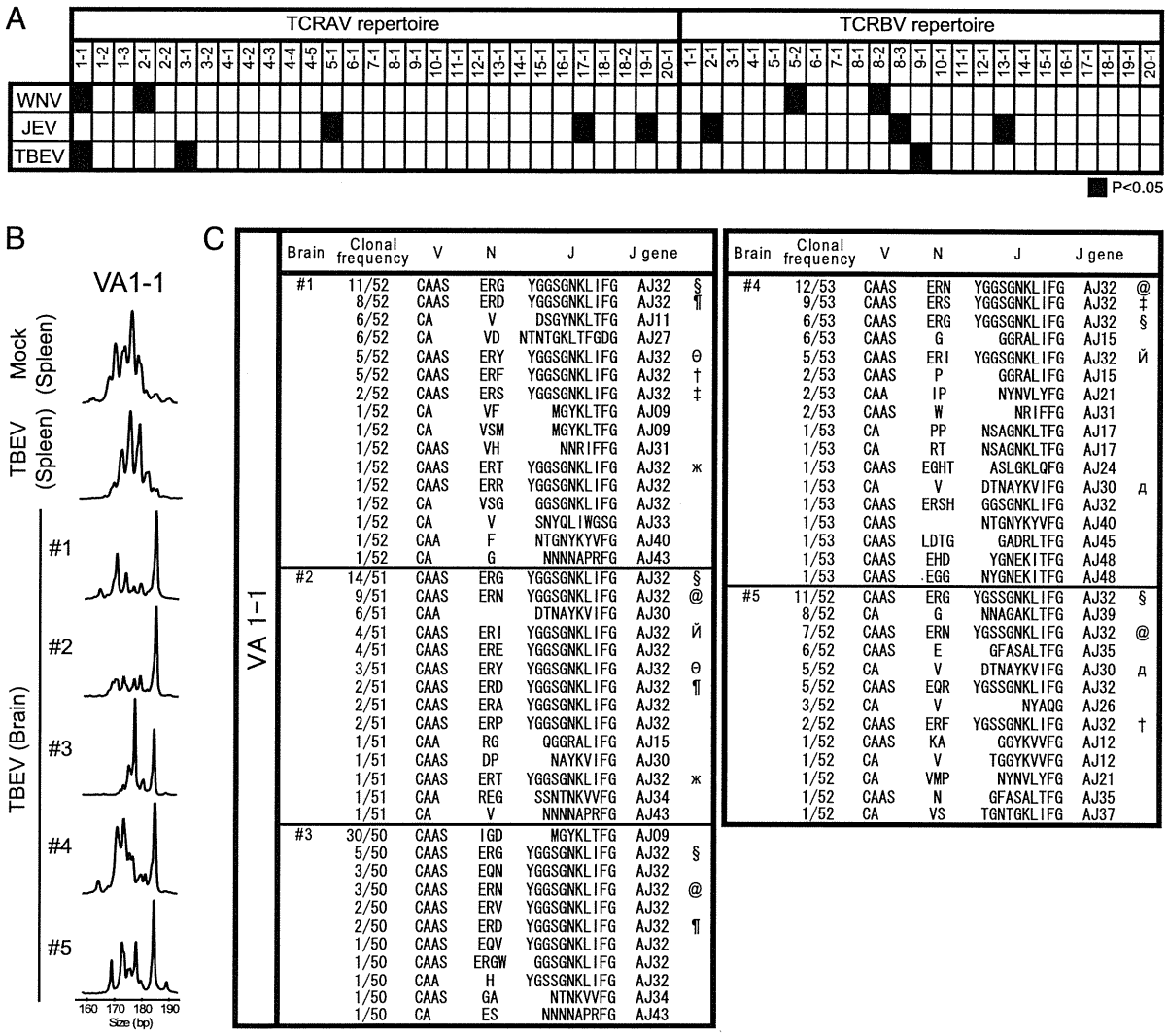

Brain	Clonal frequency	V	N	J	J gene	
#1	11/52	CAAS	ERG	YGGSGNKLIFG	AJ32	§
	8/52	CAAS	ERD	YGGSGNKLIFG	AJ32	¶
	6/52	CA	V	DSGYNKLTFG	AJ11	
	6/52	CA	VD	NTNTGKLTFGDG	AJ27	
	5/52	CAAS	ERY	YGGSGNKLIFG	AJ32	Θ
	5/52	CAAS	ERF	YGGSGNKLIFG	AJ32	†
	2/52	CAAS	ERS	YGGSGNKLIFG	AJ32	‡
	1/52	CA	VF	MGYKLTFG	AJ09	
	1/52	CA	VSM	MGYKLTFG	AJ09	
	1/52	CAAS	VH	NNRIFFG	AJ31	
	1/52	CAAS	ERT	YGGSGNKLIFG	AJ32	Ж
	1/52	CAAS	ERR	YGGSGNKLIFG	AJ32	
	1/52	CA	VSG	GGSGNKLIFG	AJ32	
	1/52	CA	V	SNYQLIWGSG	AJ33	
	1/52	CAA	F	NTGNYKYVFG	AJ40	
	1/52	CA	G	NNNNAPRFG	AJ43	
#2	14/51	CAAS	ERG	YGGSGNKLIFG	AJ32	§
	9/51	CAAS	ERN	YGGSGNKLIFG	AJ32	@
	6/51	CAA		DTNAYKVIFG	AJ30	
	4/51	CAAS	ERI	YGGSGNKLIFG	AJ32	Й
	4/51	CAAS	ERE	YGGSGNKLIFG	AJ32	
	3/51	CAAS	ERY	YGGSGNKLIFG	AJ32	Θ
	2/51	CAAS	ERD	YGGSGNKLIFG	AJ32	¶
	2/51	CAAS	ERA	YGGSGNKLIFG	AJ32	
	2/51	CAAS	ERP	YGGSGNKLIFG	AJ32	
	1/51	CAA	RG	QGGRALIFG	AJ15	
	1/51	CAAS	DP	NAYKVIFG	AJ30	
	1/51	CAAS	ERT	YGGSGNKLIFG	AJ32	Ж
	1/51	CAA	REG	SSNTNKVVFG	AJ34	
	1/51	CA	V	NNNNAPRFG	AJ43	
#3	30/50	CAAS	IGD	MGYKLTFG	AJ09	
	5/50	CAAS	ERG	YGGSGNKLIFG	AJ32	§
	3/50	CAAS	EQN	YGGSGNKLIFG	AJ32	
	3/50	CAAS	ERN	YGGSGNKLIFG	AJ32	@
	2/50	CAAS	ERV	YGGSGNKLIFG	AJ32	
	2/50	CAAS	ERD	YGGSGNKLIFG	AJ32	¶
	1/50	CAAS	EQV	YGGSGNKLIFG	AJ32	
	1/50	CAAS	ERGW	GGSGNKLIFG	AJ32	
	1/50	CAA	H	YGSSGNKLIFG	AJ32	
	1/50	CAAS	GA	NTNKVVFG	AJ34	
	1/50	CA	ES	NNNNAPRFG	AJ43	

Brain	Clonal frequency	V	N	J	J gene	
#4	12/53	CAAS	ERN	YGGSGNKLIFG	AJ32	@
	9/53	CAAS	ERS	YGGSGNKLIFG	AJ32	‡
	6/53	CAAS	ERG	YGGSGNKLIFG	AJ32	§
	6/53	CAAS	G	GGRALIFG	AJ15	
	5/53	CAAS	ERI	YGGSGNKLIFG	AJ32	Й
	2/53	CAAS	P	GGRALIFG	AJ15	
	2/53	CAA	IP	NYNVLYFG	AJ21	
	2/53	CAAS	W	NRIFFG	AJ31	
	1/53	CA	PP	NSAGNKLTFG	AJ17	
	1/53	CA	RT	NSAGNKLTFG	AJ17	
	1/53	CAAS	EGHT	ASLGKLQFG	AJ24	
	1/53	CA	V	DTNAYKVIFG	AJ30	Д
	1/53	CAAS	ERSH	GGSGNKLIFG	AJ32	
	1/53	CAAS		NTGNYKYVFG	AJ40	
	1/53	CAAS	LDTG	GADRLTFG	AJ45	
	1/53	CAAS	EHD	YGNEKITFG	AJ48	
	1/53	CAAS	EGG	NYGNEKITFG	AJ48	
#5	11/52	CAAS	ERG	YGSSGNKLIFG	AJ32	§
	8/52	CA	G	NNAGAKLTFG	AJ39	
	7/52	CAAS	ERN	YGSSGNKLIFG	AJ32	@
	6/52	CAAS	E	GFASALTFG	AJ35	
	5/52	CA	V	DTNAYKVIFG	AJ30	Д
	5/52	CAAS	EQR	YGSSGNKLIFG	AJ32	
	3/52	CA	V	NYAQG	AJ26	
	2/52	CAAS	ERF	YGSSGNKLIFG	AJ32	†
	1/52	CAAS	KA	GGYKVVFG	AJ12	
	1/52	CA	V	TGGYKVVFG	AJ12	
	1/52	CA	VMP	NYNVLYFG	AJ21	
	1/52	CAAS	N	GFASALTFG	AJ35	
	1/52	CA	VS	TGNTGKLIFG	AJ37	

FIGURE 6. Comparison of TCR repertoires of brain-infiltrating T lymphocytes among WNV-, JEV-, and TBEV-infected mice. *A*, TCRAV and TCRBV repertoires, which were increased in the brains by infection with WNV, JEV, or TBEV, are indicated by filled boxes ($p < 0.05$, Student unpaired t test, $n = 5$). TCR repertoire of T cells in JEV-infected mouse brains was reported previously (7). *B*, CDR3 size spectratyping of T cells bearing VA1-1 in TBEV-infected mouse brains. *C*, Amino acid sequences of CDR3 regions of VA1-1 in TBEV-infected mouse brains. Identical sequences detected in different individual mice are marked by the symbols.

TBEV-, and JEV-infected mice, with the exception of VA1-1, which increased significantly in WNV as well as TBEV (Fig. 6*A*). T cell clonality was examined in TBEV-infected mice brain, with a VA1-1–specifc primer by CDR3 size spectratyping (Fig. 6*B*). Oligoclonal peak patterns of T cells were detected in all five TBEV-infected mice. A dominant peak was identical in length among five mice. However, the length of the dominant peak was different between WNV- and TBEV-infected mice brain (Figs. 3*B*, 6*B*).

To examine whether these expanding T cells shared identical or similar TCR repertoires between WNV- and TBEV-infected mice, the nucleotide sequences of CDR3 were determined for VA1-1 cDNA clones from TBEV-infected mice (Fig. 6*C*). Nine clonotypes (CAAS-ERX-YGGSGNKLIFG; X of N region including G, D, Y, F, S, T, N, and I; and CA-V-DTNAYKVIFG) were detected in different mice. These clonotypes had highly similar CDR3 sequences and differed in a single amino acid residue within the N region. Additionally, preferential usage of AJ32 was observed in VA1-1 of the TBEV-infected brains. However, there was no similarity in CDR3 sequences between clonotypes obtained from WNV-infected and TBEV-infected mice. These results indicated that the brain-infiltrating T cells induced by closely related viruses, namely WNV, JEV, and TBEV, did not use shared TCR repertoires.

Cross-reaction of brain-infiltrating T cells between WNV and JEV in vitro

The specificity and cross-reactivity of brain-infiltrating T cells were examined. T cells isolated from either WNV- or JEV-infected C3H/HeN (H-2k) mouse brains were cultured for 12 h with PECs infected with WNV or JEV. Levels of IFN-γ and TNF-α were assessed by ELISA in the culture supernatant fluids (Table II). High levels of IFN-γ and TNF-α were detected in the supernatants of T cells from WNV-infected mouse brains after stimulation with WNV-infected PECs of C3H/HeN mice, but not after stimulation with JEV-infected PECs of C3H/HeN mice or WNV-infected PECs from mice with different MHC haplotypes. High IFN-γ and TNF-α production was also detected in the supernatants of T cells from JEV-infected mouse brains only after stimulation with JEV-infected PECs of C3H/HeN mice. Additionally, in vitro stimulation of $CD4^+$ or $CD8^+$ cells isolated separately from WNV-infected mouse brain was performed (Table III). The results

Table II. IFN-γ and TNF-α production by T cells isolated from WNV- or JEV-infected C3H/HeN mouse brains after in vitro stimulation with WNV or JEV

PECs Isolated from	Virus Infection	IFN-γ Production (pg/ml)		TNF-α Production (pg/ml)	
		T Cells Isolated from WNV-Infected C3H/HeN Mice Brain	T Cells Isolated from JEV-Infected C3H/HeN Mice Brain	T Cells Isolated from WNV-Infected C3H/HeN Mice Brain	T Cells Isolated from JEV-Infected C3H/HeN Mice Brain
C3H/HeNJcl (H-2^k)	WNV	1446.6 ± 55.5	20.3 ± 8.5	476.9 ± 46.7	26.4 ± 9.8
	JEV	18.7 ± 3.1	1038.2 ± 53.4	19.8 ± 7.2	370.1 ± 84.1
	None	18.3 ± 4.5	17.5 ± 6.5	22.7 ± 3.1	25.2 ± 4.9
C57BL/6JJcl (H-2^b)	WNV	24.1 ± 7.2	22.1 ± 4.4	21.9 ± 6.1	25.3 ± 7.4
	JEV	26.3 ± 8.6	24.7 ± 3.9	19.2 ± 4.3	24.2 ± 5.4
	None	25.0 ± 6.5	20.1 ± 4.2	23.3 ± 5.9	26.2 ± 6.2
BALB/cAJcl (H-2^d)	WNV	15.7 ± 2.5	21.1 ± 7.1	27.2 ± 8.4	24.1 ± 4.7
	JEV	18.9 ± 3.6	23.7 ± 5.8	26.3 ± 6.0	24.4 ± 1.2
	None	23.3 ± 7.5	24.7 ± 2.2	27.0 ± 9.1	29.6 ± 3.3

Levels of IFN-γ and TNF-α were assessed by ELISA in the supernatants of T cells isolated from WNV- or JEV-infected mouse brains ($n = 8$) after in vitro stimulation for 12 h with PECs infected with WNV or JEV. Numbers indicate the mean ± SD of IFN-γ and TNF-α production (pg/ml) in triplicate wells.

indicate that $CD8^+$ cells isolated from the brains of mice infected with WNV were virus-specific, but not cross-reactive, between WNV and JEV, and that $CD4^+$ T cells were not WNV-specific.

T cells from WNV-infected mouse brains were cultured with PECs infected with WNV for 3 d. CDR3 sequences of VA1-1 and VA2-1 were compared before and after in vitro stimulation (Table IV). Before stimulation, the pooled T cells exhibited oligoclonality with several TCR clonotypes that were identical to the dominant TCR clonotypes found in five individual mice in Fig. 5. After stimulation for 3 d, the T cells also showed extensive clonality for both VA1-1 and VA2-1 (Table IV). The dominant CDR3 sequences were maintained after stimulation, suggesting the expansion of specific T cell clones.

Discussion

WNV (strain NY99-6922) induced encephalitis in C3H/HeN mice after i.p. administration. Histopathological analysis demonstrated encephalitic changes, CNS degeneration, and infiltration of $CD3^+$ $CD8^+$ T cells in the brains of WNV-infected mice. This corresponds to the fact that the expression level of CD3 and CD8 positively correlated with viral RNA levels in the brains of WNV-infected mice. These results suggest that $CD8^+$ T cells predominantly infiltrated in the brains as infection progressed. It has been reported that tissue destruction and the presence of $CD3^+$ $CD8^+$ T cells were found in the brains of JEV- and TBEV-infected mice (7, 24). There are reports on human T cell responses following in vitro stimulation of PBMCs from WNV-infected patients with peptides derived from WNV Ags (25, 26). They indicated a critical role of $CD8^+$ T cells and IFN-γ production in responses to a limited number of epitopes with MHC restriction. The similar nature of T cell immunity between humans and mice supports the idea that the murine model in the present study is useful for elucidating the characteristics of brain-infiltrating T cells during flavivirus infection. This will lead to greater understanding of T cell immune responses in WNV-infected humans.

$CD4^+$ cells were stained and their transcripts were persistently expressed at a high level in both mock and infected mouse brains. This is probably due to the presence of microglia that express CD4 in CNS resident cells (27, 28). These results do not necessarily mean that $CD4^+$ T cells are absent in the WNV-infected brains. It has been reported that both $CD4^+$ and $CD8^+$ T cells increase in the brains after WNV infection (29). The CD4 transcripts expressed by the microglia, which are abundantly present in the CNS, might mask more $CD4^+$ T cells in the brains. Notably, the expression level of the contents of cytotoxic granules, such as perforin, granzyme A, and granzyme B, were positively related to the increase in CD8 in the brain. These cytotoxicity-related genes were mainly expressed in activated $CD8^+$ cells or NK cells, but not in $CD4^+$ cells. It is known that $CD8^+$ T cells are activated separately from NK cells in WNV-infected mouse brains (30). These results suggest that most of the brain-infiltrating T lymphocytes are cytotoxic $CD8^+$ T cells.

Th1-type cytokines were largely induced in the brains in response to WNV infection. The increased expression of IFN-γ, TNF-α, and IL-2 were remarkable on day 10 after viral infection, suggesting that Th1 cytokine-producing T cells contribute to antiviral response in the CNS. It is of interest that IL-10 was abundantly expressed in both the spleens and brains. A recent report demonstrated that IL-10 was mainly produced by $CD4^+$ cells and was dramatically elevated in WNV-infected mice (31). Given that IL-10 controls host immune responses by suppressing Th1 responses (32), elevated production of IL-10 impacts on WNV

Table III. IFN-γ and TNF-α production by $CD8^+$ cells, but not $CD4^+$ cells, isolated from WNV-infected C3H/HeN mouse brains after in vitro stimulation with WNV- or JEV-infected PECs in C3H/HeN mice

C3H/HeN PECs Infected with	Isolated Cells from WNV-Infected C3H/HeN Mice Brain			
	IFN-γ Production (pg/ml)		TNF-α Production (pg/ml)	
	$CD4^+$ Cells	$CD8^+$ Cells	$CD4^+$ Cells	$CD8^+$ Cells
WNV	15.4 ± 4.2	1358.1 ± 74.5	26.4 ± 3.9	623.6 ± 49.2
JEV	17.1 ± 4.7	19.8 ± 8.2	23.9 ± 5.8	23.1 ± 6.1
None	16.6 ± 6.1	24.7 ± 6.9	24.1 ± 7.7	28.5 ± 2.7

Levels of IFN-γ and TNF-α were assessed by ELISA in supernatants of $CD4^+$ or $CD8^+$ cells isolated from WNV-infected mouse brains ($n = 8$) after in vitro stimulation for 12 h with PECs infected with WNV or JEV. Numbers indicate the mean ± SD of IFN-γ and TNF-α production (pg/ml) in three wells.

Table IV. T cell clonalities in WNV-infected mouse brains before and after in vitro stimulation with PECs infected with WNV

Clonal Frequency	V	N	J	J Gene[a]	Frequency[b]
VA1-1 (prestimulation)					
12/55	CAVS	IG	NSGTYQRFG	AJ13 #	2/5
10/55	CAVS	LA	NSGTYQRFG	AJ13 $	1/5
8/55	CAVS	MG	NSGTYQRFG	AJ13 §	3/5
7/55	CAVS	KG	NSGTYQRFG	AJ13 †	2/5
6/55	CAV	RPT	ASLGKLQFG	AJ24 ‡	1/5
4/55	CAVS	PG	NSGTYQRFG	AJ13	2/5
4/55	CAVS		TNAYKVIFG	AJ30	0/5
2/55	CAVS	RG	NSGTYQRFG	AJ13	1/5
1/55	CAVS	RG	QGGRALIFG	AJ15	1/5
1/55	CAVS	MG	GYQNFYFG	AJ49	2/5
VA1-1 (poststimulation)[d]					
37/52	CAVS	IG	NSGTYQRFG	AJ13 #	2/5
10/52	CAVS	MG	NSGTYQRFG	AJ13 §	3/5
3/52	CAVS	KG	NSGTYQRFG	AJ13 †	2/5
1/52	CAVS	LA	NSGTYQRFG	AJ13 $	1/5
1/52	CAV	RPT	ASLGKLQFG	AJ24 ‡	1/5
VA2-1 (prestimulation)[c]					
14/51	CAAS	EA	GNYKYVFG	AJ40 #	4/5
11/51	CAAS	EG	GNYKYVFG	AJ40 $	2/5
7/51	CAAS	G	GSALGRLHFG	AJ18	1/5
6/51	CAA	RG	NNYAQGLTFG	AJ26 §	1/5
4/51	CAAS	VA	GNYKYVFG	AJ40 †	1/5
3/51	CAAS	G	NNYAQGLTFG	AJ26	1/5
2/51	CAAS	NA	NAYKVIFG	AJ30	1/5
2/51	CAA	I	TGGNNKLTFG	AJ56	1/5
1/51	CA	PRG	NNYAQGLTFG	AJ26	1/5
1/51	CAAS	P	TNAYKVIFG	AJ30	1/5
VA2-1 (poststimulation)[d]					
35/54	CAAS	EG	GNYKYVFG	AJ40 $	2/5
16/54	CAAS	EA	GNYKYVFG	AJ40 #	4/5
2/54	CAA	RG	NNYAQGLTFG	AJ26 §	1/5
1/54	CAAS	VA	GNYKYVFG	AJ40 †	1/5

[a]Identical sequences observed in both pre- and poststimulation are marked by respective symbols in the column.
[b]The frequency indicates the number of mice, among a total of five, where the clones with the respective CDR3 sequences were detected in Fig. 5.
[c]T cells were isolated from eight WNV-infected C3H/HeN mouse brains and pooled (n = 8). CDR3 regions of cDNA clones containing VA1-1 and VA2-1 were sequenced.
[d]T cells were stimulated in vitro with PECs infected with WNV at 37°C for 3 d and were subjected to CDR3 sequence analysis.

pathogenesis by preventing the host from inducing a hyperinflammatory immune reaction. It is known that chemokines and chemokine receptors are important to the pathogenesis of WNV infection. Microglia and astrocytes secrete the chemokines CCL5 and CXCL10 (33), which recruit effector T cells via the chemokine receptors CXCR3 (19, 34) and CCR5 (29) in C57BL/6J mice, respectively. The expression levels of the chemokines CCL5 and CXCL10 increased >100-fold in the brains, whereas the increases in their receptors, CCR5 and CXCR3, were not as pronounced in C3H mice. As has been previously reported (35), the expression levels of early (CD25) and late (CD69) T cell activation markers were increased with time. Thus, it is likely that the brain-infiltrating T lymphocytes are mostly supplied by local expansion of $CD8^+$ T cells, rather than by the recruitment of $CCR5^+$ or $CXCR3^+$ T cells across the blood–brain barrier by the CCL5 and CXCL10.

TCR mRNA was below detectable levels in the mock brains because of poor infiltration of T cells. In contrast, TCR expression was ~100-fold higher in WNV-infected brains on day 10 compared with mock-infected brains. There is a possibility that the accumulation of T cells in the brains is caused by nonspecific migration from peripheral organs and random leakage from peripheral blood. However, the T cells showed high oligoclonality in their TCR repertoires that were completely different between WNV-infected mice and JEV-infected mice. Moreover, a few T cells that resided within the brains increased drastically from day 7 to day 10. These results suggest that the increase in the number of $CD8^+$ T cells in the brains is mainly due to local expansion of T cells that recognize different Ags among closely related viruses.

TCR usage was found to be completely different between WNV- and JEV-infected mice brains; this is not, however, consistent with cross-reactivity of Abs between WNV and JEV (15). MHC-restricted cytotoxic T cells against WNV-infected target cells were detected in mice (36, 37), and mouse spleen cells immunized with JEV partially lysed WNV-infected target cells (38, 39). Peptide variants derived from 9-aa residues of NS4b elicit cross-reactive $CD8^+$ T cells in both JEV and WNV, whereas their functional and phenotypic properties were different between JEV and WNV (40). In our studies, the brain-infiltrating $CD8^+$ T cells showed a similar characteristic, namely a Th1/Tc1 phenotype, between WNV- and JEV-infected mice. $CD8^+$ T cells isolated from virus-infected mouse brains produced IFN-γ and TNF-α after coculture in vitro with virus-infected PECs with syngeneic

MHC haplotype, suggesting that the CD8$^+$ T cells within brains are virus-specific and not cross-reactive with other flaviviruses. Moreover, dominant T cells with a high clonality were detected in the brains of different individual mice, suggesting that they were not induced by bystander activation of nonspecific T cells. These results strongly suggest that the dominant T cells elicited in brains by in vivo primary WNV infection are virus-specific and not crossreactive. It is possible that the cross-reactive T cells are subdominant in the brain following primary WNV infection. Cellular cloning techniques or sequential stimulation in vitro with Ag probably induce a skewed hierarchy of T cells and may not be genuinely representative of the in vivo T cell populations. The direct cloning of TCR genes from local inflammatory sites would be a powerful tool for understanding T cell-mediated immunopathology and recovery in WNV encephalitis.

CDR3 sequence analysis revealed interesting results on Ag specificity. Most TCR clonotypes obtained from the brains of flavivirus-infected mice showed preferential usage of AJ segments (AJ13 for VA1-1 of WNV, AJ40 for VA2-1 of WNV, AJ32 for VA1-1 of TBEV). For WNV-infected mice, TCR clonotypes derived from VA1-1 contained rich hydrophobic amino acids such as alanine, glycine, isoleucine, leucine, methionine, and proline in the N region (126 of 154 residues). TBEV-infected mice frequently used an ERX motif (for glutamate, arginine, and X, which represents any amino acid), which contains polar amino acids in the N region. The dissimilarity in CDR3α sequences suggests the expansion of T cells with different Ag specificities between WNV-infected mice and TBEV-infected mice. The brain-infiltrating T lymphocytes did not share identical TCR repertoires between WNV-infected and JEV-infected mice (7).

In contrast to the very restricted TCRAV repertoire, the brain-infiltrating T lymphocytes exhibited relatively broad TCRBV repertoires. In VB5-2, CDR3 sequences varied considerably among individual mice, although BJ usage was limited to BJ2.1 and BJ2.7. Similarly, a common CDR3 sequence was not found in VB8-2 among individual mice. This contrasting result probably reflects a different role of TCR α- and β-chains in Ag recognition. The difference in the extent of repertoire restriction between TCR α- and β-chains has been shown in mice infected with JEV, a closely related flavivirus (7). Usage of restricted TCRAV and broad TCRBV has been reported in infection with other viruses, such as herpesvirus (41). Moreover, several reports have also described a dominant and essential role of the TCR α-chain in Ag recognition by T cells (42–44). It has been reported that TCRαβ heterodimers bearing a restricted TCR α-chain and diverse TCR β-chains have the potential to specifically recognize a single Ag in vitro (45). The dominant role of TCR α-chain is reflected to the restriction of the TCR β-chain repertoire observed in the brain-infiltrating T lymphocytes of WNV-infected mice.

We defined day 10 as the humane endpoint because this WNV-infected encephalitis mouse model was produced by administration of a lethal dose of the virus. Therefore, we could not observe CD8$^+$ T cell immune responses at later time points in animals that had recovered or not. It is known that the mortality rate is higher in CD8KO mice than in control mice and that CD8$^+$ T cells within the brain could play a protective role in the hosts (5). We recently reported that T cells that migrated into the brain following administration of a low dose of TBEV were different between living and dying mice (46). Further studies are needed to clarify the protective or immunopathological role of CD8$^+$ T cells by using low-dose administration of WNV.

In conclusion, Th1-like cytotoxic CD8$^+$ T cells with high clonality infiltrate into the brains of WNV-infected mice. These oligoclonal brain-infiltrating T cells use unique TCR repertoires, which are generated by a limited TCRα and diverse TCRβ genes. Moreover, the dominant brain-infiltrating CD8$^+$ T cells elicited in vivo by primary WNV infection are virus-specific, but not cross-reactive, among related flaviviruses. The present study provides important information on Ag specificity and diversity of WNV-specific CD8$^+$ T cells, as well as a new insight into the critical role of brain-infiltrating T cells in the recovery from WNV infection.

Acknowledgments

We thank Hiro Yamada and Tokikazu Nagaoka (Clinical Research Center, National Sagamihara Hospital) for assistance with our assay. We also thank Dr. Soichi Nukuzuma (Kobe Institute of Health, Kobe, Hyogo, Japan) for supplying a standard density of in vitro-synthesized WN virus NY99 RNA.

Disclosures

The authors have no financial conflicts of interest.

References

1. Petersen, L. R., and A. A. Marfin. 2002. West Nile virus: a primer for the clinician. *Ann. Intern. Med.* 137: 173–179.
2. Petersen, L. R., and J. T. Roehrig. 2001. West Nile virus: a reemerging global pathogen. *Emerg. Infect. Dis.* 7: 611–614.
3. Watson, J. T., P. E. Pertel, R. C. Jones, A. M. Siston, W. S. Paul, C. C. Austin, and S. I. Gerber. 2004. Clinical characteristics and functional outcomes of West Nile fever. *Ann. Intern. Med.* 141: 360–365.
4. Dauphin, G., S. Zientara, H. Zeller, and B. Murgue. 2004. West Nile: worldwide current situation in animals and humans. *Comp. Immunol. Microbiol. Infect. Dis.* 27: 343–355.
5. Shrestha, B., and M. S. Diamond. 2004. Role of CD8$^+$ T cells in control of West Nile virus infection. *J. Virol.* 78: 8312–8321.
6. Purtha, W. E., N. Myers, V. Mitaksov, E. Sitati, J. Connolly, D. H. Fremont, T. H. Hansen, and M. S. Diamond. 2007. Antigen-specific cytotoxic T lymphocytes protect against lethal West Nile virus encephalitis. *Eur. J. Immunol.* 37: 1845–1854.
7. Fujii, Y., K. Kitaura, K. Nakamichi, T. Takasaki, R. Suzuki, and I. Kurane. 2008. Accumulation of T-cells with selected T-cell receptors in the brains of Japanese encephalitis virus-infected mice. *Jpn. J. Infect. Dis.* 61: 40–48.
8. Davis, M. M. 1990. T cell receptor gene diversity and selection. *Annu. Rev. Biochem.* 59: 475–496.
9. Ding, Y. H., K. J. Smith, D. N. Garboczi, U. Utz, W. E. Biddison, and D. C. Wiley. 1998. Two human T cell receptors bind in a similar diagonal mode to the HLA-A2/Tax peptide complex using different TCR amino acids. *Immunity* 8: 403–411.
10. Gotoh, A., Y. Hamada, N. Shiobara, K. Kumagai, K. Seto, T. Horikawa, and R. Suzuki. 2008. Skew in T cell receptor usage with polyclonal expansion in lesions of oral lichen planus without hepatitis C virus infection. *Clin. Exp. Immunol.* 154: 192–201.
11. Matsutani, T., K. Shiiba, T. Yoshioka, Y. Tsuruta, R. Suzuki, T. Ochi, T. Itoh, H. Musha, T. Mizoi, and I. Sasaki. 2004. Evidence for existence of oligoclonal tumor-infiltrating lymphocytes and predominant production of T helper 1/T cytotoxic 1 type cytokines in gastric and colorectal tumors. *Int. J. Oncol.* 25: 133–141.
12. Shiobara, N., Y. Suzuki, H. Aoki, A. Gotoh, Y. Fujii, Y. Hamada, S. Suzuki, N. Fukui, I. Kurane, T. Itoh, and R. Suzuki. 2007. Bacterial superantigens and T cell receptor β-chain-bearing T cells in the immunopathogenesis of ulcerative colitis. *Clin. Exp. Immunol.* 150: 13–21.
13. Kitaura, K., K. Kanayama, Y. Fujii, N. Shiobara, K. Tanaka, I. Kurane, S. Suzuki, T. Itoh, and R. Suzuki. 2009. T cell receptor repertoire in BALB/c mice varies according to tissue type, sex, age, and hydrocortisone treatment. *Exp. Anim.* 58: 159–168.
14. Matsutani, T., T. Ohmori, M. Ogata, H. Soga, T. Yoshioka, R. Suzuki, and T. Itoh. 2006. Alteration of T-cell receptor repertoires during thymic T-cell development. *Scand. J. Immunol.* 64: 53–60.
15. Lim, C. K., T. Takasaki, A. Kotaki, and I. Kurane. 2008. Vero cell-derived inactivated West Nile (WN) vaccine induces protective immunity against lethal WN virus infection in mice and shows a facilitated neutralizing antibody response in mice previously immunized with Japanese encephalitis vaccine. *Virology* 374: 60–70.
16. Takashima, I., K. Morita, M. Chiba, D. Hayasaka, T. Sato, C. Takezawa, A. Igarashi, H. Kariwa, K. Yoshimatsu, J. Arikawa, and N. Hashimoto. 1997. A case of tick-borne encephalitis in Japan and isolation of the the virus. *J. Clin. Microbiol.* 35: 1943–1947.
17. Hayasaka, D., L. Ivanov, G. N. Leonova, A. Goto, K. Yoshii, T. Mizutani, H. Kariwa, and I. Takashima. 2001. Distribution and characterization of tick-borne encephalitis viruses from Siberia and far-eastern Asia. *J. Gen. Virol.* 82: 1319–1328.
18. Kasahara, T., T. Miyazaki, H. Nitta, A. Ono, T. Miyagishima, T. Nagao, and T. Urushidani. 2006. Evaluation of methods for duration of preservation of RNA quality in rat liver used for transcriptome analysis. *J. Toxicol. Sci.* 31: 509–519.

19. Klein, R. S., E. Lin, B. Zhang, A. D. Luster, J. Tollett, M. A. Samuel, M. Engle, and M. S. Diamond. 2005. Neuronal CXCL10 directs $CD8^+$ T-cell recruitment and control of West Nile virus encephalitis. *J. Virol.* 79: 11457–11466.
20. Matsutani, T., T. Yoshioka, Y. Tsuruta, S. Iwagami, and R. Suzuki. 1997. Analysis of TCRAV and TCRBV repertoires in healthy individuals by microplate hybridization assay. *Hum. Immunol.* 56: 57–69.
21. Tsuruta, Y., S. Iwagami, S. Furue, H. Teraoka, T. Yoshida, T. Sakata, and R. Suzuki. 1993. Detection of human T cell receptor cDNAs (α, β, γ and δ) by ligation of a universal adaptor to variable region. *J. Immunol. Methods* 161: 7–21.
22. Yoshida, R., T. Yoshioka, S. Yamane, T. Matsutani, T. Toyosaki-Maeda, Y. Tsuruta, and R. Suzuki. 2000. A new method for quantitative analysis of the mouse T-cell receptor V region repertoires: comparison of repertoires among strains. *Immunogenetics* 52: 35–45.
23. Horiuchi, T., M. Hirokawa, Y. Kawabata, A. Kitabayashi, T. Matsutani, T. Yoshioka, Y. Tsuruta, R. Suzuki, and A. B. Miura. 2001. Identification of the T cell clones expanding within both $CD8^+CD28^+$ and $CD8^+CD28^-$ T cell subsets in recipients of allogeneic hematopoietic cell grafts and its implication in post-transplant skewing of T cell receptor repertoire. *Bone Marrow Transplant.* 27: 731–739.
24. Hayasaka, D., N. Nagata, Y. Fujii, H. Hasegawa, T. Sata, R. Suzuki, E. A. Gould, I. Takashima, and S. Koike. 2009. Mortality following peripheral infection with tick-borne encephalitis virus results from a combination of central nervous system pathology, systemic inflammatory and stress responses. *Virology* 390: 139–150.
25. Lanteri, M. C., J. W. Heitman, R. E. Owen, T. Busch, N. Gefter, N. Kiely, H. T. Kamel, L. H. Tobler, M. P. Busch, and P. J. Norris. 2008. Comprehensive analysis of West Nile virus-specific T cell responses in humans. *J. Infect. Dis.* 197: 1296–1306.
26. Parsons, R., A. Lelic, L. Hayes, A. Carter, L. Marshall, C. Evelegh, M. Drebot, M. Andonova, C. McMurtrey, W. Hildebrand, et al. 2008. The memory T cell response to West Nile virus in symptomatic humans following natural infection is not influenced by age and is dominated by a restricted set of $CD8^+$ T cell epitopes. *J. Immunol.* 181: 1563–1572.
27. Omri, B., P. Crisanti, F. Alliot, M. C. Marty, J. Rutin, C. Levallois, A. Privat, and B. Pessac. 1994. CD4 expression in neurons of the central nervous system. *Int. Immunol.* 6: 377–385.
28. Alliot, F., M. C. Marty, D. Cambier, and B. Pessac. 1996. A spontaneously immortalized mouse microglial cell line expressing CD4. *Brain Res. Dev. Brain Res.* 95: 140–143.
29. Glass, W. G., J. K. Lim, R. Cholera, A. G. Pletnev, J. L. Gao, and P. M. Murphy. 2005. Chemokine receptor CCR5 promotes leukocyte trafficking to the brain and survival in West Nile virus infection. *J. Exp. Med.* 202: 1087–1098.
30. Liu, Y., R. V. Blanden, and A. Müllbacher. 1989. Identification of cytolytic lymphocytes in West Nile virus-infected murine central nervous system. *J. Gen. Virol.* 70: 565–573.
31. Bai, F., T. Town, F. Qian, P. Wang, M. Kamanaka, T. M. Connolly, D. Gate, R. R. Montgomery, R. A. Flavell, and E. Fikrig. 2009. IL-10 signaling blockade controls murine West Nile virus infection. *PLoS Pathog.* 5: e1000610.
32. Moore, K. W., R. de Waal Malefyt, R. L. Coffman, and A. O'Garra. 2001. Interleukin-10 and the interleukin-10 receptor. *Annu. Rev. Immunol.* 19: 683–765.
33. Cheeran, M. C., S. Hu, W. S. Sheng, A. Rashid, P. K. Peterson, and J. R. Lokensgard. 2005. Differential responses of human brain cells to West Nile virus infection. *J. Neurovirol.* 11: 512–524.
34. Zhang, B., Y. K. Chan, B. Lu, M. S. Diamond, and R. S. Klein. 2008. CXCR3 mediates region-specific antiviral T cell trafficking within the central nervous system during West Nile virus encephalitis. *J. Immunol.* 180: 2641–2649.
35. Wang, Y., M. Lobigs, E. Lee, and A. Müllbacher. 2003. $CD8^+$ T cells mediate recovery and immunopathology in West Nile virus encephalitis. *J. Virol.* 77: 13323–13334.
36. Kesson, A. M., R. V. Blanden, and A. Mullbacher. 1987. The primary in vivo murine cytotoxic T cell response to the flavivirus, West Nile. *J. Gen. Virol.* 68: 2001–2006.
37. Uren, M. F., P. C. Doherty, and J. E. Allan. 1987. Flavivirus-specific murine $L3T4^+$ T cell clones: induction, characterization and cross-reactivity. *J. Gen. Virol.* 68: 2655–2663.
38. Hill, A. B., A. Müllbacher, C. Parrish, G. Coia, E. G. Westaway, and R. V. Blanden. 1992. Broad cross-reactivity with marked fine specificity in the cytotoxic T cell response to flaviviruses. *J. Gen. Virol.* 73: 1115–1123.
39. Murali-Krishna, K., V. Ravi, and R. Manjunath. 1994. Cytotoxic T lymphocytes raised against Japanese encephalitis virus: effector cell phenotype, target specificity and in vitro virus clearance. *J. Gen. Virol.* 75: 799–807.
40. Trobaugh, D. W., L. Yang, F. A. Ennis, and S. Green. 2010. Altered effector functions of virus-specific and virus cross-reactive $CD8^+$ T cells in mice immunized with related flaviviruses. *Eur. J. Immunol.* 40: 1315–1327.
41. Dong, L., P. Li, T. Oenema, C. L. McClurkan, and D. M. Koelle. 2010. Public TCR use by herpes simplex virus-2-specific human CD8 CTLs. *J. Immunol.* 184: 3063–3071.
42. Dietrich, P. Y., F. A. Le Gal, V. Dutoit, M. J. Pittet, L. Trautman, A. Zippelius, I. Cognet, V. Widmer, P. R. Walker, O. Michielin, et al. 2003. Prevalent role of TCR α-chain in the selection of the preimmune repertoire specific for a human tumor-associated self-antigen. *J. Immunol.* 170: 5103–5109.
43. Messaoudi, I., J. LeMaoult, B. M. Metzner, M. J. Miley, D. H. Fremont, and J. Nikolich-Zugich. 2001. Functional evidence that conserved TCR CDRα3 loop docking governs the cross-recognition of closely related peptide:class I complexes. *J. Immunol.* 167: 836–843.
44. Trautmann, L., N. Labarrière, F. Jotereau, V. Karanikas, N. Gervois, T. Connerotte, P. Coulie, and M. Bonneville. 2002. Dominant TCR Vα usage by virus and tumor-reactive T cells with wide affinity ranges for their specific antigens. *Eur. J. Immunol.* 32: 3181–3190.
45. Yokosuka, T., K. Takase, M. Suzuki, Y. Nakagawa, S. Taki, H. Takahashi, T. Fujisawa, H. Arase, and T. Saito. 2002. Predominant role of T cell receptor (TCR)-α chain in forming preimmune TCR repertoire revealed by clonal TCR reconstitution system. *J. Exp. Med.* 195: 991–1001.
46. Fujii, Y., D. Hayasaka, K. Kitaura, T. Takasaki, R. Suzuki, and I. Kurane. 2011. T cell clones expressing different T cell receptors accumulate in the brains of dying and surviving mice following peripheral infection with tick-borne encephalitis virus. *Viral Immunol.* In press.

VIRAL IMMUNOLOGY
Volume 24, Number 4, 2011

Pp. 1–12
DOI: 10.1089/vim.2011.0017

T-Cell Clones Expressing Different T-Cell Receptors Accumulate in the Brains of Dying and Surviving Mice After Peripheral Infection with Far Eastern Strain of Tick-Borne Encephalitis Virus

Yoshiki Fujii,[1,2] Daisuke Hayasaka,[3] Kazutaka Kitaura,[1,2]
Tomohiko Takasaki,[1] Ryuji Suzuki,[2] and Ichiro Kurane[1]

Abstract

Tick-borne encephalitis virus (TBEV), a representative acute central nervous system disease-inducible virus, is known to elicit dose-independent mortality in a mouse model. We previously reported that subcutaneous infection with a wide range of TBEV Oshima strain challenge doses (10^2–10^6 PFU) produced an approximately 50% mortality rate. However, the factors playing critical roles in mortality and severity remain unclear. In this study, we distinguished surviving and dying mice by their degree of weight loss after TBEV infection, and investigated qualitative differences in brain-infiltrating T cells between each group by analyzing T-cell receptor (TCR) repertoire and complementary determining region 3 (CDR3) sequences. TCR repertoire analysis revealed that the expression levels of VA8-1, VA15-1, and VB8-2 families were increased in brains derived from both surviving and dying mice. CDR3 amino acid sequence characteristics differed between each group. In dying mice, high frequencies of VA15-1/AJ12 and VB8-2/BJ1.1 gene usage were observed. While in surviving mice, high frequencies of VA8-1/AJ15 or VA8-1/AJ23 gene usage were observed. VB8-2/BJ2.7 gene usage and short CDR3 were observed frequently in both surviving and dying mice. However, no differences in T-cell activation markers and apoptosis-related genes were observed between these groups using quantitative real-time PCR analysis. These results suggest that TBEV-infection severity may be involved in antigen specificity, but not in the number or activation level of brain-infiltrating T cells.

Introduction

Tick-borne encephalitis virus (TBEV) is a positive-sense single-stranded RNA virus of the family Flaviviridae that also includes Japanese encephalitis virus (JEV), West Nile virus (WNV), St. Louis encephalitis virus, and Murray Valley encephalitis virus. TBEV is an important causative agent of acute central nervous system disease in humans (8, 27). TBEV is distributed widely throughout Europe and Asia, and is genetically divided into three closely-related subtypes: the European, Siberian, and Far Eastern subtypes (9,20). The Far Eastern subtype is also distributed in southern parts of Hokkaido, Japan (38–40).

Clinical manifestations caused by TBEV range from inapparent infections and fevers, with complete recovery of patients, to debilitating or fatal encephalitis. While such diverse manifestations can be caused by any of the three subtypes (16,17), the percentage of severe cases differs among each subtype. We previously reported that differences exist in the severity of symptoms among individual mice after peripheral infection with the Oshima strain of TBEV, a member of the Far Eastern subtype (6,18,21). Following subcutaneous infection with a wide range of challenge doses (10^2–10^6 PFU), the mortality rate was consistently approximately 50% (21). Although a dose-independent mortality pattern is shown in several encephalitic flavivirus infection models, the causative biological mechanisms have yet to be defined (24,26,35,42,44,45). Thus, we investigated the immunological and biological responses in surviving and dying mice, so that increased corticosteroid serum levels and TNF-α

[1]Department of Virology 1, National Institute of Infectious Diseases, Tokyo, Japan.
[2]Department of Rheumatology and Clinical Immunology, Clinical Research Center for Allergy and Rheumatology, Sagamihara National Hospital, National Hospital Organization, Sagamihara, Japan.
[3]Department of Virology, Institute of Tropical Medicine, Nagasaki University, Nagasaki, Japan.

expression levels in the serum and the brains were observed in dying mice (21). However, as there was no significant difference in viral loads and the levels of cellular infiltration in the brains between the two groups, the fate of infected mice was not likely to be determined by neuro-invasiveness or the number of brain-infiltrating cells.

Multiple complex factors are associated with encephalitis pathogenesis. Recent studies indicate that brain-infiltrating T cells play an important role in viral encephalitis (24,26,34,45). T cells potentially contribute to both recovery and immunopathogenesis, and the functional balance between these differs among virus species and experimental conditions. For example, it is widely thought that T-cell responses are essential for viral clearance in WNV infection (4,5,15,32,36,37), although differences in responses between surviving and dying mice under identical inoculation conditions have not been determined. We further reported no differences in the number of brain-infiltrating $CD8^+$ T cells in our previous study (21), but did not compare immunological markers.

We previously demonstrated that T cells with selected T-cell receptors (TCRs) accumulate in JEV-infected mouse brains using TCR repertoire analysis and nucleotide sequencing of the complementary determining region 3 (CDR3) (10). These are efficient methods for analyzing relative expression levels of each TCR family and the frequency of each T-cell clone, which allows us to better understand the pathological and/or protective mechanism in our TBEV-infected mouse model. By determining the TCR repertoire and frequencies of T-cell clones we can assess if different patterns exist between surviving and dying mice. Identical patterns would indicate that disease severity is independent of T cells, whereas different patterns would indicate that T-cell antigen recognition pattern is related to severity. The purpose of our study was therefore to clarify whether T cells influence the severity of TBEV-induced encephalitis.

Materials and Methods

Virus and cells

Stock virus of TBEV Oshima 5-10 strain (accession no. AB062063) was prepared from the medium used to culture baby hamster kidney (BHK) cells after five passages through suckling mouse brains (20). BHK cells were maintained in Eagle's Minimal Essential Medium (EMEM; Nissui Pharmaceutical Co., Tokyo, Japan) containing 8% fetal calf serum (FCS). All experiments using live TBEV were performed in a biosafety level three (BSL3) laboratory at the Tokyo Metropolitan Institute for Neuroscience according to the standard BSL3 guidelines.

Mice

Five-week old female C57BL/6j mice were subcutaneously inoculated with 10^3 PFU of TBEV diluted in EMEM containing 2% FCS. Mock-infected mice were inoculated with EMEM from the supernatant medium of BHK cells. Mice were weighed daily and observed for clinical disease symptoms including behavioral symptoms and signs of paralysis. Morbidity was determined as relative weight loss compared with day 0. Thirteen days post-infection (dpi), mice exhibiting more than 25% or less than 10% weight loss were recognized as dying or surviving mice, respectively (21). The Animal Care and Use Committee of the Tokyo Metropolitan Institute for Neuroscience approved all experimental protocols.

Isolation of total RNA from tissues

Mice injected with mock or TBEV were anesthetized and perfused with cold PBS at 13 dpi. Brains and spleens were excised and immediately submerged in RNA*later*® RNA Stabilization Reagent (Qiagen, Hilden, Germany). Total RNA was then isolated using an RNeasy Lipid Tissue Mini kit (Qiagen) according to the manufacturer's instructions. Isolated total RNA was used for TCR repertoire analysis, CDR3 sequencing, and quantification of viral RNA and gene expressions using quantitative real-time PCR.

Adaptor ligation-mediated polymerase chain reaction (AL-PCR)

AL-PCR methodology was previously reported (30,41,48). Briefly, isolated total RNA was converted to double-stranded cDNA using the Superscript cDNA synthesis kit (Invitrogen, Carlsbad, CA), according to the manufacturer's instructions, except that a specific primer (BSL-18E) was used (48). The P10EA/P20EA adaptors were ligated to the 5′ end of cDNA and this adaptor-ligated cDNA was cut with *Sph* I. PCR was performed using TCR α-chain or β-chain constant region-specific primers (MCA1 or MCB1) and P20EA. The second PCR was performed with MCA2 or MCB2 and P20EA. Biotinylation of PCR products was performed using both P20EA and 5′-biotinylated MCA3 or MCB3 primers.

TCR repertoire analysis

TCRAV and TCRBV repertoires were analyzed using a microplate hybridization assay (MHA) (48). In brief, 10 pmol of amino-modified oligonucleotides specific for TCRAV and TCRBV segments were immobilized onto carboxylate-modified 96-well microplates with water-soluble carbodiimide. Prehybridization and hybridization were performed in GMCF buffer (0.5 M Na_2HPO_4, pH 7.0, 1 mM EDTA, 7% SDS, 1% BSA, and 7.5% formamide) at 47°C. One-hundred microliters of denatured 5′-biotinylated PCR products were mixed with an equivalent volume of 0.4 N NaOH/10 mM EDTA, and added to 10 mL of GMCF buffer. Hybridization solution (100 μL) was added to each well of the microplate containing immobilized oligonucleotide probes specific for the V segment. After hybridization, the wells were washed four times with washing buffer (2×SSC, 0.1% SDS) at room temperature. The plate was incubated at 37°C for 10 min for stringency washing. After washing four times with 2×SSC, 0.1% SDS, 200 μL of TB-TBS buffer (10 mM Tris-HCl, 0.5 M NaCl, pH 7.4, 0.5% Tween 20, and 0.5% blocking reagent; Boehringer Mannheim, Mannheim, Germany) were added to block non-specific binding. Next, 100 μL of 1:1000-diluted alkaline phosphatase-conjugated streptavidin in TB-TBS was added, and the sample was incubated at 37°C for 30 min. The plates were washed six times in T-TBS (10 mM Tris-HCl, 0.5 M NaCl, pH 7.4, and 0.5% Tween 20). For color development, 100 μL of substrate solution (4 mg/mL p-nitrophenylphosphate in 10% diethanolamine, pH 9.8) was added and the absorbance was determined at 405 nm. The ratio of the hybridization intensity for each TCRV-specific

probe to that of a TCRC-specific probe (V/C value) was determined using the TCR cDNA concentrated samples that contained the corresponding V segment and the universal C segment, respectively. Absorbances obtained for each TCRV-specific probe were divided by the corresponding V/C value. The relative frequency was calculated using the corrected absorbencies by the formula: relative frequency (%) = (corrected absorbance of TCRV-specific probe/the sum of corrected absorbencies of TCRV-specific probes)×100.

T-cell clonality analysis with CDR3 size spectratyping

PCR was performed for CDR3 size spectratyping (23) for 30 cycles in a 20 μL volume under the same conditions as described above. PCR assays used 1 μL of 1:20 or 1:50 diluted second PCR product, 0.1 μM of 5′-Cy5 MCA3/MCB3 primer, and 0.1 μM of the primer specific for each variable segment. Oligonucleotide probes for hybridization were used as primers specific for each variable segment (as described above). Two microliters of 1:20-diluted PCR product in sample loading solution was analyzed using a CEQ8000 Genetic Analysis System (Beckman Coulter, Brea, CA). Spleen cells from mock-infected mice were used as a control for the peak patterns of peripheral blood.

Determination of nucleotide sequence of CDR3 regions

PCR was performed with 1 μL of 1:20 diluted second PCR product, using a forward primer specific to the variable region and a reverse primer specific to the constant region (MCA4 or MCB4) under the conditions described above. Primers VA8-1 (5′-ACGCCACTCTCCATAAGAGCA-3′), VA15-1 (5′-GTGGACAGAAAACAGAGCCAA-3′), and VB8-2 (5′-GGCTACCCCCTCTCAGACAT-3′) were used in this study. After elution from the agarose gel, PCR products were cloned into the pGEM-T Easy Vector (Promega Corp., Madison, WI). DH5α-competent cells were transformed with the

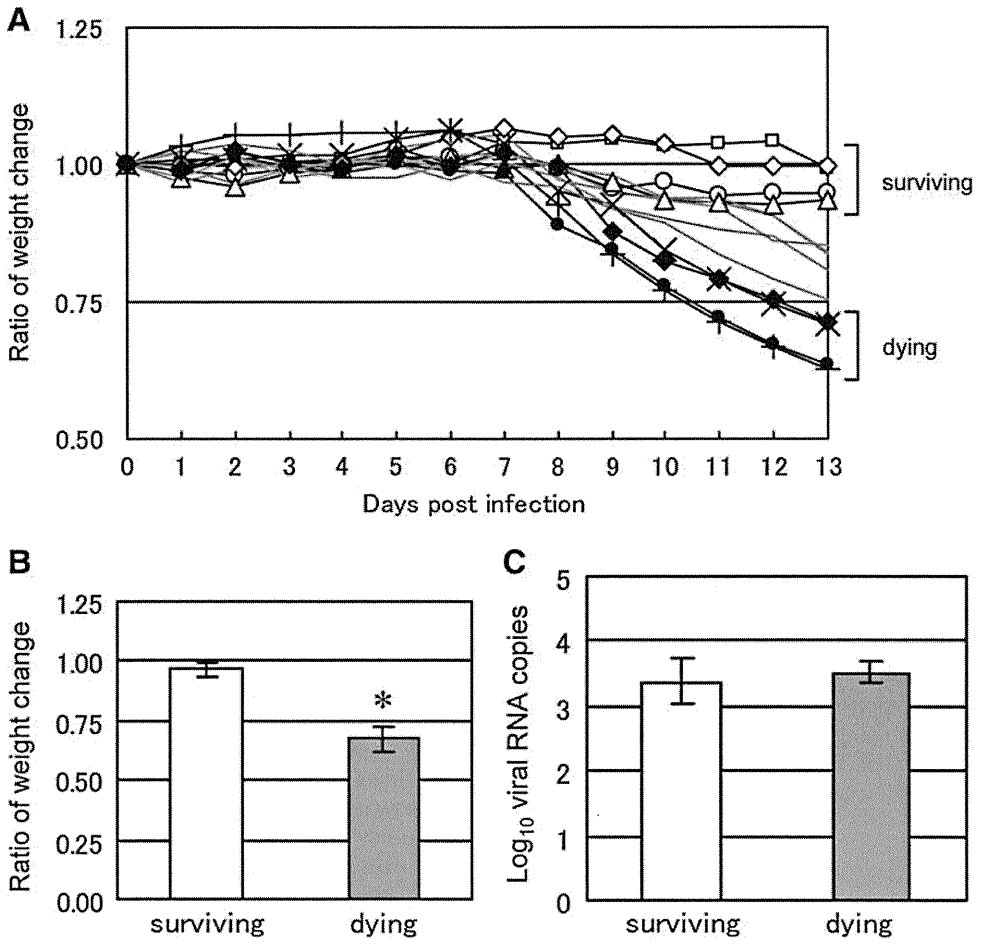

FIG. 1. Fatality of TBEV-infected mice is characterized by weight loss rather than brain viral replication. (**A**) Individual daily weight changes of TBEV-infected mice. Mice were monitored daily for signs of disease, and the ratio of weight change of individuals at each time point was compared with those at day 0 and recorded following subcutaneous infection with TBEV Oshima strain (10^3 PFU) in C57BL/6 mice (n = 13). Individuals with intermediate weight loss (10–25%) at 13 dpi are shown as gray lines, and mock-infected mice are not shown. (**B**) Average weight change ratios for surviving (ratio of weight change >0.90) and dying (<0.75) mouse groups at 13 dpi (n = 4). Error bars represent standard deviations. Asterisk indicates statistically significant ($p < 0.05$) differences between surviving and dying mice by Student's *t*-test. (**C**) Quantification of viral RNA in brains at 13 dpi. qPCR was performed using primers specific for TBEV NS1. Viral RNA copy number per 1 ng of total RNA is shown (n = 4). Statistically significant differences were not observed between surviving and dying mice.

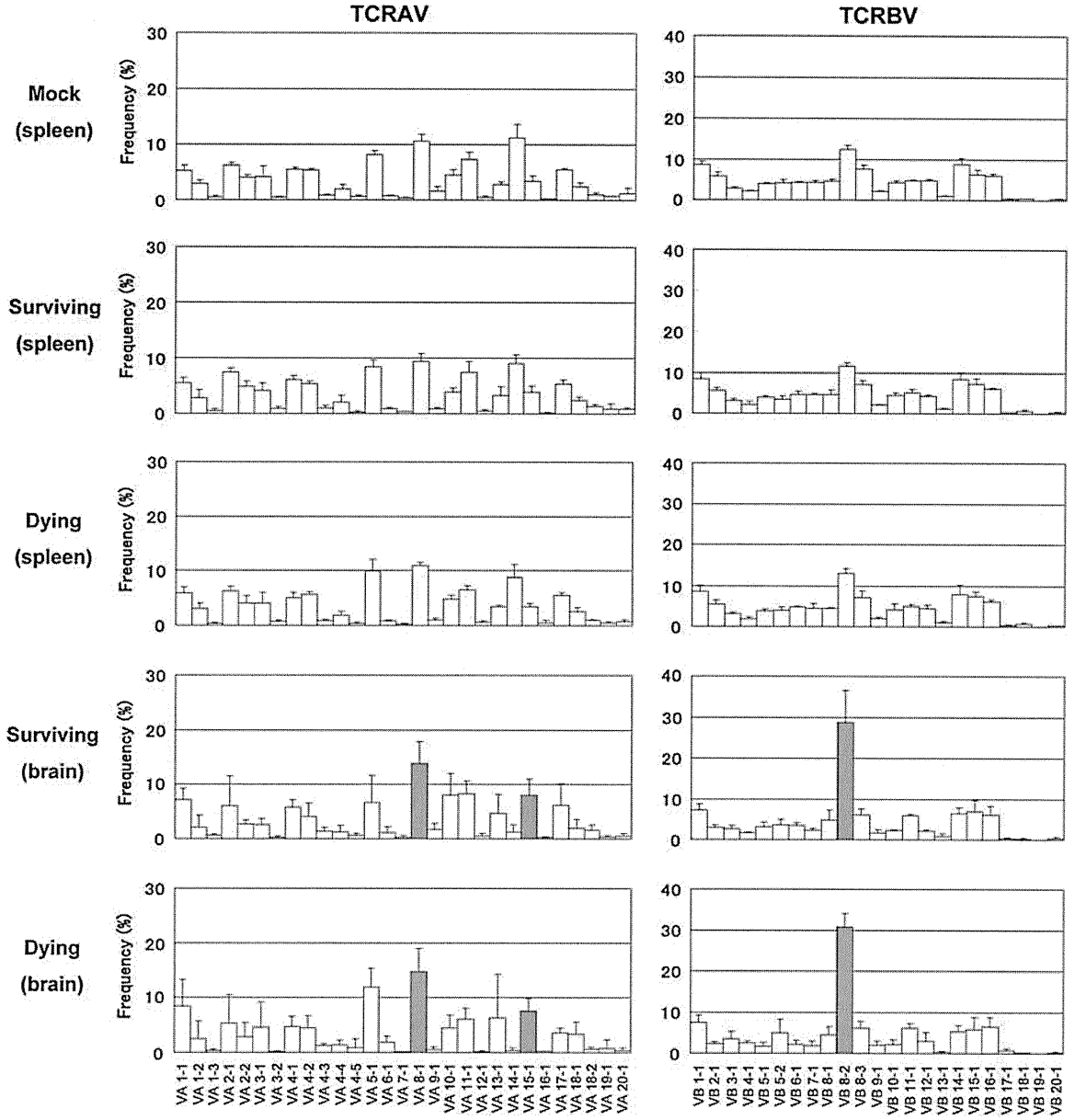

FIG. 2. TCR repertoire analysis of spleens and brains from TBEV-infected or mock-infected mice. TCRAV and TCRBV repertoires were analyzed by MHA as described in the materials and methods section. Mean percent frequencies ± SD (standard deviation) of 4 mice are indicated. Gray bars indicate a significant increase compared with mock-infected spleens ($p < 0.05$ by Student's t-test).

recombinant plasmid DNA. Sequence reactions were performed with a GenomeLab DTCS Quick Start Kit (Beckman Coulter) and analyzed using the CEQ8000 Genetic Analysis System (Beckman Coulter).

Quantitative real-time PCR (qPCR)

mRNA expression levels of T-cell-related antigens, activation markers, and apoptosis-related genes for brains excised from TBEV-infected or mock-infected mice were determined by qPCR using a LightCycler (Roche Diagnostics Corp., Indianapolis, IN). Previously reported primer pairs specific for glyceraldehyde-3-phosphate dehydrogenase (GAPDH), CD3, CD4, and CD8 (10) were used in this study. The following additional primer pairs were designed for our study: CD25 (forward: 5′-AAGATGAAGTGTGGGAAAA CGG-3′, reverse: 5′-GGGAAGTCTGTGGTGGTTATGG-3′), CD69 (forward: 5′-AGGATCCATTCAAGTTTCTATCCC-3′, reverse: 5′-CAACATGGTGGTCAGATGATTCC-3′), Granzyme (Gym) A (forward: 5′-CCTGAAGGAGGCTGT GAAAG-3′, reverse: 5′-GAGTGAGCCCCAAGAATGAA-3′), Gym B (forward: 5′-CCATCGTCCCTAGAGCTGAG-3′, reverse: 5′-TTGTGGAGAGGGCAAACTTC-3′), Perforin (forward: 5′- GCCTGGTACAAAAACCTCCA-3′, reverse: 5′-AGGGCTGTAAGGACCGAGAT-3′) and Fas ligand (FasL) (forward: 5′- GGGCAGTATTCAATCTTACCAG-3′, reverse: 5′-GTGCCCATGATAAAGAATAGTAGA-3′). Freshly isolated RNA was converted to cDNA using a PrimeScript™ RT

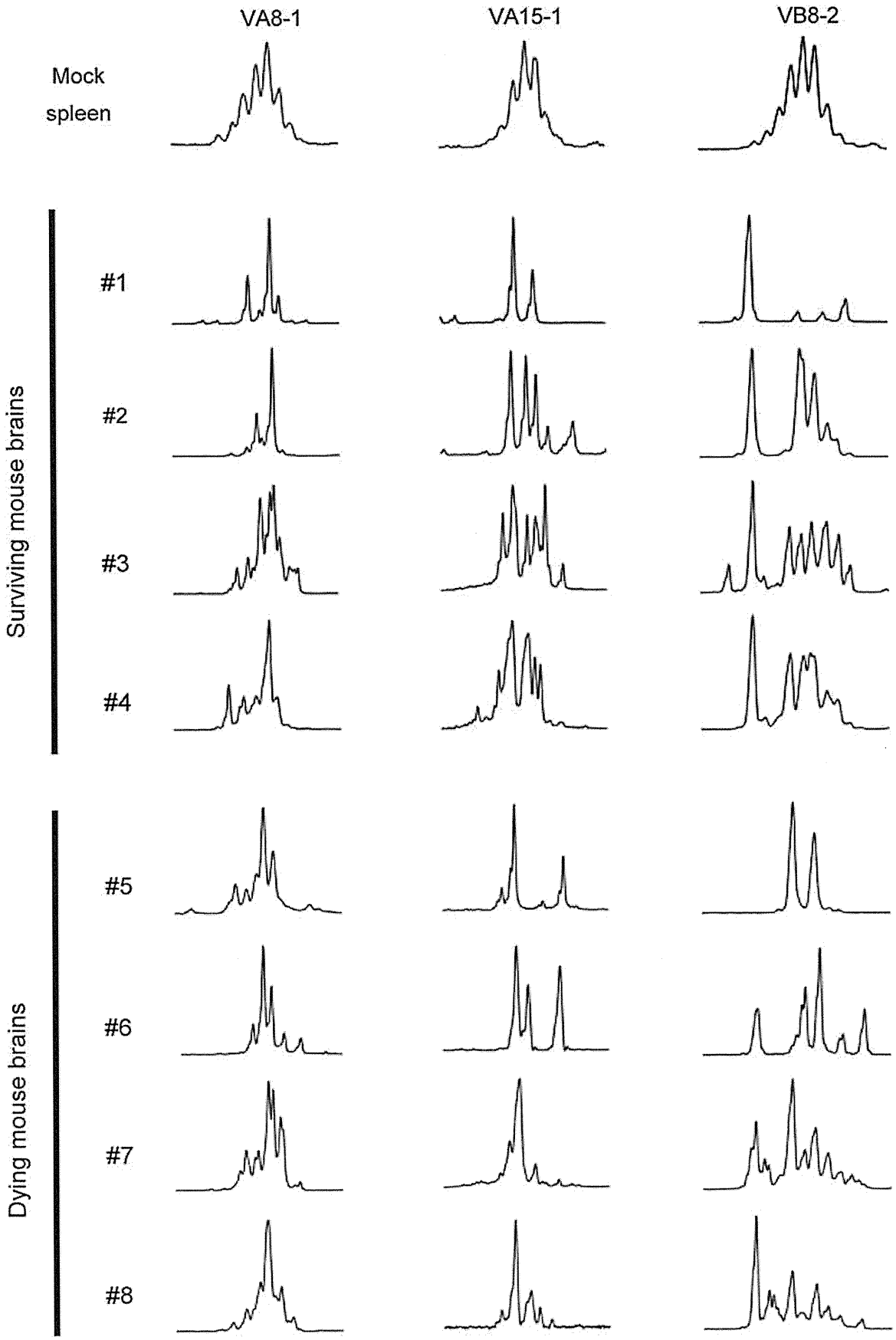

FIG. 3. CDR3 size spectratyping revealed different T-cell clonality patterns between surviving and dying mice. T-cell clonality for VA8-1, VA15-1, and VB8-2 families in individual mouse brains are shown. Peak numbers indicate the size variation of CDR3. Nucleotide size becomes longer at the right side. Generally, multiple peaks indicate the existence of polyclonal T cells, and one or a few peaks indicate the existence of monoclonal and oligoclonal T cells, respectively. Mock-infected spleen was used as a control to indicate polyclonal pattern.

A

AV8-1 (surviving mice)

mouse	freq.	CDR3 V	N	J	J gene	
#1	3/12	CALS	DLVT	NTGKLTF	AJ27	[§]
	3/12	CALR	AHY	NQGKLIF	AJ23	†
	3/12	CALT	PNY	NQGKLIF	AJ23	[‡]
	1/12	CALS	PNY	NQGKLIF	AJ23	[†]
	1/12	CALR	PNY	NQGKLIF	AJ23	†
	1/12	CALG	PNY	NQGKLIF	AJ23	†
#2	8/11	CALS	HYQ	GGRALIF	AJ15	[*]
	3/11	CAL	KGS	SGNKLIF	AJ32	
#3	2/15	CALS	LAY	NQGKLIF	AJ23	†
	2/15	CALS	ASSS	GSWQLIF	AJ22	
	2/15	CALR	GQ	GGRALIF	AJ15	*
	2/15	CAL	KGY	NQGKLIF	AJ23	†
	1/15	CAC	KGY	NQGKLIF	AJ23	†
	1/15	CALS	EGY	NQGKLIF	AJ23	†
	1/15	CALS	PNY	NQGKLIF	AJ23	[†]
	1/15	CALT	PNY	NQGKLIF	AJ23	[‡]
	1/15	CALS	DLVT	NTGKLTF	AJ27	[§]
	1/15	CALS	GTSG	GNYKPTF	AJ6	
	1/15	CAL	IRGS	ALGRLHF	AJ18	
#4	6/13	CALS	HYQ	GGRALIF	AJ15	[*]
	3/13	CAL	W	MGYKLTF	AJ9	
	1/13	CALS	EPS	GSWQLIF	AJ22	
	1/13	CALS	VTG	SGGKLTF	AJ44	
	1/13	CAL	AGY	NQGKLIF	AJ23	†
	1/13	CA	ST	GYQNFYF	AJ49	

AV8-1 (dying mice)

mouse	freq.	CDR3 V	N	J	J gene	
#5	5/11	CA	RN	SNNRIFF	AJ31	
	3/11	CALS	PNY	NQGKLIF	AJ23	[†]
	2/11	CALS	LN	YAQGLTF	AJ26	
	1/11	CA	STTA	SLGKLQF	AJ24	
#6	5/13	CALS	EGG	SNAKLTF	AJ42	
	5/13	CAL	YTE	GADRLTF	AJ45	
	2/13	CALS	GY	NQGKLIF	AJ23	†
	1/13	CALS	DHSYQ	GGRALIF	AJ15	
#7	3/15	CALS	DGG	TGSKLSF	AJ58	
	2/15	CALR	P	GYQNFYF	AJ49	
	2/15	CALS	PNY	NQGKLIF	AJ23	[†]
	1/15	CALS	QNY	NQGKLIF	AJ23	†
	1/15	CALS	Y	NQGKLIF	AJ23	†
	1/15	CALS	DGT	GGYKVVF	AJ12	
	1/15	CALS	GT	GGYKVVF	AJ12	
	1/15	CALS	VG	SNYQLIW	AJ33	
	1/15	CALR	LTSG	GNYKPTF	AJ6	
	1/15	CALS	DQTA	SLGKLQF	AJ24	
	1/15	CALR	SSYQ	GGRALIF	AJ15	
#8	3/12	CALS	ERN	YAQGLTF	AJ26	
	2/12	CALS	EGG	MGYKLTF	AJ9	
	2/12	CALR	RSP	GYQNFYF	AJ49	
	1/12	CAL	VNY	NQGKLIF	AJ23	†
	1/12	CAL	NTGG	LSGKLTF	AJ2	
	1/12	CALR	GS	AGNKLTF	AJ17	
	1/12	CA	ATS	SGQKLVF	AJ16	
	1/12	CA	WN	SNNRIFF	AJ31	

B

VA15-1 (surviving mice)

mouse	freq.	CDR3 V	N	J	J gene	
#1	4/15	CAAS	MDY	NQGKLIF	AJ23	
	11/15	CAAG	N	AGAKLTF	AJ39	
#2	5/14	CAAS	TGA	NTGKLTF	AJ52	
	3/14	CAAK	EA	SNYQLIW	AJ33	[§]
	3/14	CAAS	IG	SNYQLIW	AJ33	
	2/14	CAAS	T	GYQNFYF	AJ49	
	1/14	CAAS	IWGA	NTGKLTF	AJ52	
#3	6/15	CAPG	GATA	SLGKLQF	AJ24	
	4/15	CAAT	N	YAQGLTF	AJ26	
	1/15	CAAS	WAS	GSWQLIF	AJ22	¶
	1/15	CAAS	WSS	GSWQLIF	AJ22	¶
	1/15	CAAS	TSS	GSWQLIF	AJ22	[¶]
	1/15	CAAS	S	NYNVLYF	AJ21	
	1/15	CAAG	T	GGYKVVF	AJ12	*
#4	10/14	CAAR	D	MGYKLTF	AJ9	[†]
	1/14	CAAS	P	MGYKLTF	AJ9	[‡]
	2/14	CAAK	EA	SNYQLIW	AJ33	[§]
	1/14	CAAS	TSS	GSWQLIF	AJ22	[¶]

VA15-1 (dying mice)

mouse	freq.	CDR3 V	N	J	J gene	
#5	11/13	CAAR	T	GGYKVVF	AJ12	[×]
	2/13	CAAS	GA	GGYKVVF	AJ12	[*]
#6	5/10	CAAS	GA	GGYKVVF	AJ12	[*]
	5/10	CAAS	TSS	GSWQLIF	AJ22	[¶]
#7	5/13	CAAS	GA	GGYKVVF	AJ12	[*]
	4/13	CAAS	TA	GGYKVVF	AJ12	*
	3/13	CAAS	KA	GGYKVVF	AJ12	*
	1/13	CAAR	T	GGYKVVF	AJ12	[×]
#8	7/13	CAAR	D	MGYKLTF	AJ9	[†]
	2/13	CAAS	GA	GGYKVVF	AJ12	[*]
	1/13	CAAS	DGT	GGYKVVF	AJ12	*
	1/13	CAAS	P	MGYKLTF	AJ9	[‡]
	1/13	CAAS	TN	SGTYQRF	AJ13	
	1/13	CAAT	PPSS	GSWQLIF	AJ22	¶

FIG. 4. Amino acid sequences of TCR CDR3 regions of cDNA clones derived from TBEV-infected mouse brains. For the VA8-1 (**A**), VA15-1 (**B**) or VB8-2 (**C**) families, predicted amino acid sequences are shown with their frequencies of cDNA clones in each individual mouse. J gene usage is shown at the right side of each sequence. V, N (N-D-N), and J gene segments are not strictly divided. Each symbol indicates a group of identical or similar sequences, and brackets indicate an identical sequence among individuals.

C

VB8-2 (surviving mice)

mouse	freq.	CDR3 V	CDR3 N-D-N	CDR3 J	J gene	
#1	8/17	CASGD		EQYF	BJ2.7	[*]
	4/17	CASSD	APPNTG	QLYF	BJ2.2	
	3/17	CASGD	LGGRGNYA	EQFF	BJ2.1	[§]
	1/17	CASRA	PWGEGTG	QLYF	BJ2.2	
	1/17	CASGD	ASFY	EQYF	BJ2.7	
#2	4/15	CASGD	ATGY	EQYF	BJ2.7	[¶]
	3/15	CASGE	LGAY	EQYF	BJ2.7	
	3/15	CASGD	MGQKD	TQYF	BJ2.5	[£]
	2/15	CASGD	AQLSY	EQYF	BJ2.7	
	2/15	CASGD		EQYF	BJ2.7	[*]
	1/15	CASGD	AGDRGV	EVFF	BJ1.1	
#3	2/10	CASGD	LGGRGNYA	EQFF	BJ2.1	[§]
	1/10	CASGD	LWGALNQD	TQYF	BJ2.5	
	1/10	CASGV	PGQGTTG	QLYF	BJ2.2	
	1/10	CASSG	QGAGNQ	APLF	BJ1.5	
	1/10	CASSD	ATISNE	RLFF	BJ1.4	
	1/10	CASGG	TGVAE	TLYF	BJ2.3	
	1/10	CASGE	GGVGN	TLYF	BJ1.3	
	1/10	CASGS	R	EQYF	BJ2.7	*
	1/10	CASGD		EQYF	BJ2.7	[*]
#4	2/10	CASGD	VRGDS	DYTF	BJ1.2	
	1/10	CASGD	MGQKD	TQYF	BJ2.5	[£]
	1/10	CASGK	LANQD	TQYF	BJ2.5	
	1/10	CANSE	WGADHD	TQYF	BJ2.5	
	1/10	CARGD	AGGSAE	TLYF	BJ2.3	
	1/10	CASKS	IQD	TQYF	BJ2.5	
	1/10	CASGD	ATGY	EQYF	BJ2.7	[¶]
	1/10	CASGD	G	GEYF	BJ2.7	*
	1/10	CASGD		EQYF	BJ2.7	[*]

VB8-2 (dying mice)

mouse	freq.	CDR3 V	CDR3 N-D-N	CDR3 J	J gene	
#5	5/14	CASGT	PGGNT	EVFF	BJ1.1	
	3/14	CASGD	IRV	EVFF	BJ1.1	[†]
	3/14	CASGD	VRV	EVFF	BJ1.1	†
	2/14	CASGD	AWGKD	TQYF	BJ2.5	
	1/14	CASSD	APTSAE	TLYF	BJ2.3	
#6	8/13	CASGD	ATAIT	EVFF	BJ1.1	
	1/13	CASGG	DWGANTG	QLYF	BJ2.2	
	1/13	CASSD	LGVNYA	EQFF	BJ2.1	
	1/13	CASGD	NRV	EVFF	BJ1.1	[‡]
	1/13	CASGD		TQYF	BJ2.5	*
	1/13	CASGD		EQYF	BJ2.7	[*]
#7	2/13	CASGD	AGTG	EQYF	BJ2.7	
	2/13	CASGA	G	LGIF	BJ2.7	*
	1/13	CASGD	IRV	EVFF	BJ1.1	[†]
	1/13	CASGA	GST	EVFF	BJ1.1	†
	1/13	CASGG	GQKNS	DYTF	BJ1.2	
	1/13	CASGE	VGGRSA	EQFF	BJ2.1	
	1/13	CASGD	ALV	EQYF	BJ2.7	
	1/13	CASSD	AGW	EQYF	BJ2.7	
	1/13	CASGE		SEYF	BJ2.7	*
	1/13	CASGD		GPYF	BJ2.7	*
	1/13	CASGA		LEYF	BJ2.7	*
#8	3/15	CASGV	PY	EQYF	BJ2.7	
	2/15	CASGD		EQYF	BJ2.7	[*]
	1/15	CASGD	ARGNQD	TQYF	BJ2.5	
	1/15	CASGD	NRV	EVFF	BJ1.1	[‡]
	1/15	CASGE	AW	GGAF	BJ2.5	
	1/15	CASGD	AGHSY	EQYF	BJ2.7	
	1/15	CASGD	LGAD	EQYF	BJ2.7	
	1/15	CASGD	G	GEYF	BJ2.7	*
	1/15	CASGD		FQYF	BJ2.7	*
	1/15	CASGD		TLYF	BJ1.3	
	1/15	CASGD		EVFF	BJ1.1	

FIG. 4. (Continued).

reagent kit (Takara Bio Inc., Shiga, Japan), and the PCR reaction was performed using SYBR® Premix Taq™ (Takara Bio) for SYBR Green I according to the manufacturer's instructions. The expression level of each gene was measured by qPCR as demonstrated previously (10). Expression levels were normalized based on the housekeeping gene GAPDH copy number. Relative quantification was expressed as a ratio between TBEV-infected and mock-infected brains.

Viral RNA levels of TBEV were examined with NS1-specific primers (forward: 5′-CGGCTAGCCACACTATCGACAA-3′, reverse: 5′-GGCGAGTACTTCCATGGTCCTT-3′). Reverse transcription and PCR reactions were conducted as described above. Viral RNA was quantified as copy number per 1 ng of total RNA. Copy number in each sample was determined on the basis of a standard curve.

Statistical analysis

Student's *t*-test was used for statistical analysis to assess significant differences in weight change ratio, the degree of the relative expression in TCR repertoire analysis, and the expression levels of genes in qPCR analysis. The Mann-Whitney *U* test was used to evaluate frequencies of CDR3 sequences. A p value <0.05 was determined to be statistically significant.

Results

Discrimination of surviving and dying mice

Thirteen C57BL/6 mice were subcutaneously inoculated with 10^3 PFU of TBEV and weighed daily (Fig. 1A). Four mice from each of the surviving and dying groups were used in the experiments. Dying mice were defined as those exhibiting more than 25% weight loss at 13 dpi, and surviving mice were defined as those with less than 10% weight change. Mock-infected mice (n = 4) exhibited negligible weight change (data not shown). Weight percentage at 13 dpi, compared with that on day 0, was significantly different between the surviving and dying mouse groups (Fig. 1B). However, the amounts of viral RNA in the brains at the 13 dpi were no different between these two groups of mice (Fig. 1C). These data indicate that the virus propagation level is not the main factor that determines the fatality of TBEV-infected mice. ◀F1

TCR repertoire analysis

TCRAV and TCRBV repertoires were analyzed using brains and spleens collected from TBEV-infected dying mice, surviving mice, or mock-infected mice at 13 dpi (Fig. 2). Using TCR repertoire analysis, significant expressions of TCRAV and TCRBV were detected in TBEV-infected brains ◀F2

both in surviving and dying mice. Frequencies of T cells bearing VA8-1, VA15-1, and VB8-2 were significantly increased in brains compared with mock-infected spleens. However, there was no significant difference between surviving and dying mice. VA14-1, known as the family expressed on NKT cells (3), was expressed at very low levels in virus-infected brains. No difference between mock-infected and TBEV-infected mouse spleens was observed for both TCRAV and TCRBV repertoires, and this suggests that systemic T-cell response changes were below the detectable level in our analysis. In mock-infected mouse brains, the expression of TCRAV and TCRBV was not detected (data not shown) due to the low lymphocyte numbers.

CDR3 size spectratyping

We performed CDR3 size spectratyping analysis to confirm the clonalities of T cells expressing VA8-1, VA15-1, and VB8-2 families in TBEV-infected mouse brains (Fig. 3). Different patterns were observed between TBEV-infected brains and mock spleens for all three families. Furthermore, VA15-1 clonalities for dying mice were higher than those for surviving mice. A short VB8-2 size peak was also observed in surviving mice.

Amino acid sequences of CDR3

Because differences in T-cell clonality were observed between surviving and dying mice, nucleotide sequences of the CDR3 were determined for the above-mentioned TCR families, using PCR-amplified and randomly-selected cDNA clones. Predicted amino acid sequences are shown along with the frequencies of cDNA clones derived from the brains of individual mice infected with TBEV (Fig. 4). Cysteine (C) at the N-terminal portion and phenylalanine (F) or tryptophan (W) at the C-terminal portion are not contained within CDR3. Despite the fact that we analyzed more than 30 clones in mock-infected spleens, we did not find any clones with identical sequence (data not shown). Meanwhile, in TBEV-infected brains, many clones with identical sequences were found. VA8-1 (Fig. 4A) surviving mice were divided into two groups: individuals with high frequency of AJ23 gene usage (#1 and #3) or AJ15 gene usage (#2 and #4). Although dying mice also produced some clones bearing AJ23 or AJ15, the frequency of these clones was lower than in surviving mice. For VA15-1 (Fig. 4B), a high frequency of AJ12 gene usage was observed in dying mice. In addition, clones with identical amino acid sequences to CDR3 (CAAS GA GGYKVVF) were detected in all four dying mice. Identical clones bearing AJ9 and AJ22 were detected in both surviving and dying mice. For VB8-2 (Fig. 4C), a high frequency of BJ2.7 genes with short CDR3 consisting of seven amino acids (aa) was characteristic for both surviving and dying mice. Clones with such a short CDR3 were rare in TCR β chains. Some clones bearing BJ1.1 with 10 aa CDR3 (CASGD XRV EVFF, X = I, V or N) were found in every dying mouse. As shown for VA8-1, VB8-2 surviving mice were also divided into two groups: individuals (#1 and #3) that obtained clones with BJ2.1 (CASGD LGGRGNYA EQFF), or individuals (#2 and #4) that obtained clones with BJ2.7 (CASGD ATGY EQYF) and BJ2.5 (CASGD MGQKD TQYF). The frequencies of these three clones were not high in each individual, but were specific for each group. In mouse #5, there was no clone bearing BJ2.7 or short CDR3, therefore the frequency of these clones might be high but not necessary in TBEV-infected mice. As illustrated by mice #7 and #8, a high single peak in CDR3 size spectratyping analysis does not necessarily indicate monoclonal expansion. Clones were also sometimes included that were the same size as CDR3, yet had different sequences. However, several reports have shown that the β-chain J region of CDR3 does not specifically interact with antigen peptides (7,11,13,14,43). The sequence of the N-terminal half of CDR3 (V segment, D segment, and N addition) rather than J gene usage might therefore be important, as potentially each clone with a short CDR3 recognizes an identical antigen peptide. To organize sequence data, clone frequencies with more than 10% J gene usage in the total number of clones analyzed for each V family were individually plotted in Fig. 5. CDR3 length was considered for the β chain. Using the Mann-Whitney U test, the frequency of VA8-1/AJ15 was significantly higher in surviving mice, and the frequencies of VA15-1/AJ12 and VB8-2/BJ1.1 (10 aa) were significantly higher in dying mice. This suggests that these T-cell clones might be closely associated with disease severity in TBEV-infected mice.

Levels of cell surface markers and cytokines determined by qPCR

Differential patterns of T-cell clones can indicate that brain-infiltrating cells may play different roles between surviving and dying mice. To investigate the active state of the infiltrating cells, we studied the expression levels of T-cell antigen markers, lymphocyte activation markers, and apoptosis-related genes: CD3, CD4, CD8, and CD25 (expressed on activated T cells and B cells) (28), CD69 (expressed rapidly after lymphocyte activation) (47), and Gzm A, Gzm B, perforin, and FasL using qPCR analysis (Fig. 6). The resulting expression levels for all genes in TBEV-infected brains studied were significantly increased when compared with mock infection. This was especially the case for the expression of CD69, Gzm A, and Gzm B, which were increased more than 100 times. No significant differences were observed between mouse groups, indicating that equivalent $CD8^+$ T-cell infiltration into TBEV-infected brains occurs in surviving and dying mice with similar activation state levels.

Discussion

Understanding the clinical variability caused by encephalitic flavivirus infection is important in explaining differences between severe and subclinical human cases. It may also further elucidate the mechanism of pathogenesis for viral encephalitis. Previous reports showed that the TBEV Oshima strain elicited dose-independent mortality following peripheral infection in some mouse strains (6,21). We therefore distinguished surviving and dying mice by their degree of weight loss after TBEV infection according to our previous study (21), as a simple and effective method to evaluate the severity.

Based on the amount of viral RNA in brain tissue, we found no difference in virus replication between surviving and dying mice. This result suggests that direct virus-induced neuronal injury cannot completely explain the

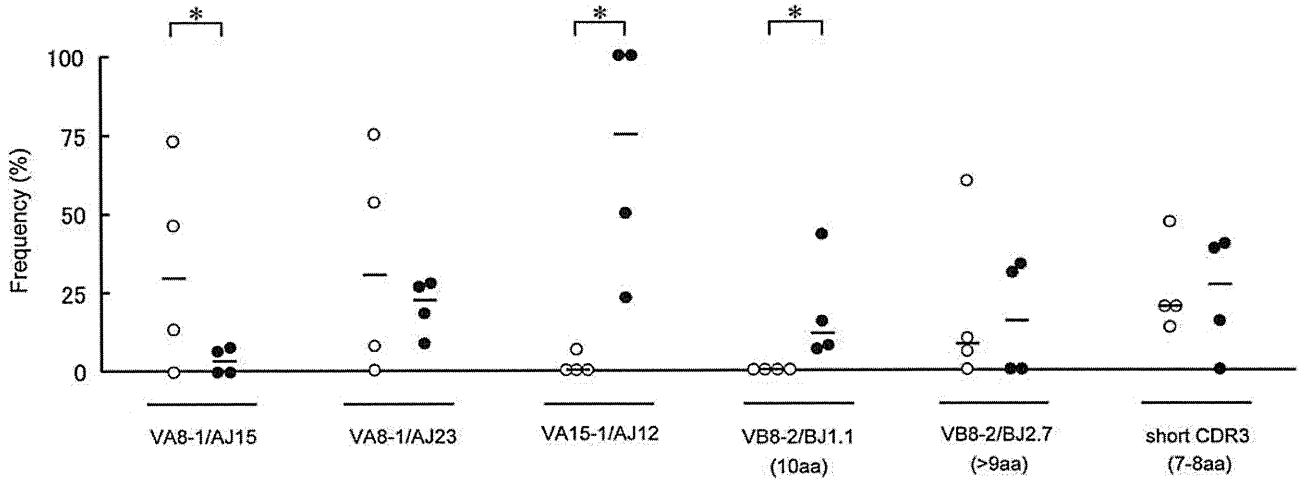

FIG. 5. Differential patterns of TCR gene usage between surviving and dying mouse brains. Frequencies for characteristic combinations of V and J gene usages were individually plotted. CDR3 length was taken into consideration for β chain: BJ2.7 (long) indicates CDR3 consisted of more than 9 aa, and short CDR3 indicates CDR3 consisted of 7 or 8 aa. Open circles indicate surviving mice, and closed circles indicate dying mice. Bars indicate the median for each group. Asterisks denote statistically significant ($p < 0.05$) differences between surviving and dying mice using the Mann-Whitney U test.

severity of TBEV infection. In our previous study (21), large numbers of $CD8^+$ T cells infiltrated the brains of TBEV-infected mice, yet no significant difference was observed between surviving and dying mice. We therefore investigated the individual characteristics of brain-infiltrating T cells in this study.

TCR repertoire analysis revealed that the frequencies of T cells bearing VA8-1, VA15-1, and VB8-2 were significantly increased in TBEV-infected mouse brains compared with those of spleens. However, there was no significant difference between surviving and dying mice. This indicated that once a certain amount of virus was inoculated, T cells with selected TCR V families accumulate in the brain regardless of disease severity. In contrast, clonality results and CDR3 sequencing analysis indicated a distinct difference between mouse groups, with frequencies of VA15-1/AJ12 and VB8-2/BJ1.1 gene usage higher in dying mice. One clone with an identical CDR3 sequence (CAAS GA GGYKVVF) was detected in all four dying mice, strongly suggesting that this clone was associated with severe encephalitis. High frequencies of VA8-1/AJ15 gene usage were characteristic of surviving mice, while high frequencies of VB8-2/BJ2.7 gene usage and clones with short CDR3 were observed in both surviving and dying mice. We therefore observed a unique increase of T-cell clones for each mouse group. Specific clones were found only in dying mice, while other clones were frequently found in surviving mice or were commonly found in every infected mouse. Thus, there are several T-cell clones that may be associated with the severity of TBEV infection, while the remaining clones may be different in

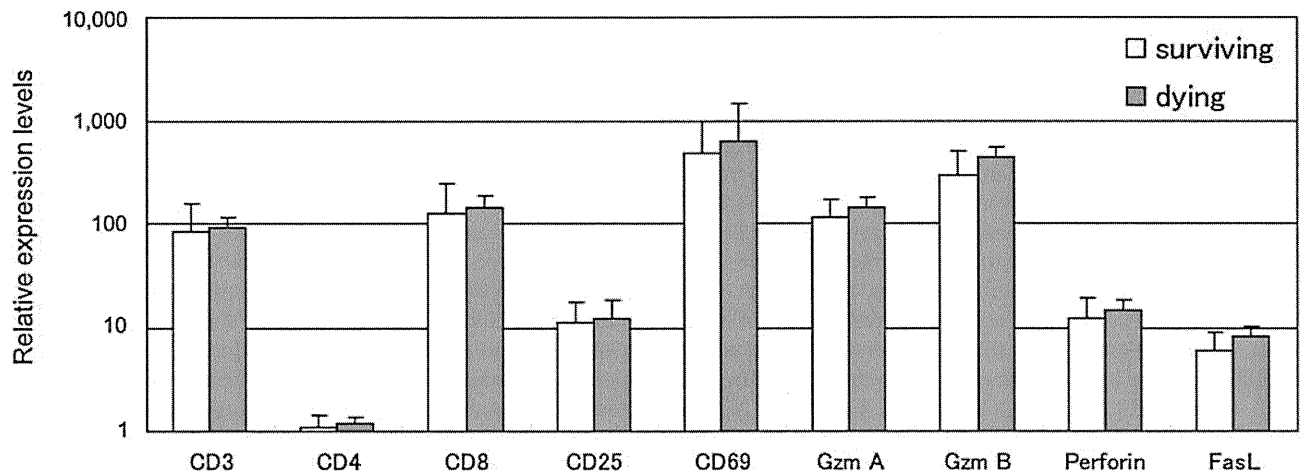

FIG. 6. Quantification of mRNA expression of T-cell-related antigens, activation markers, and apoptosis-related genes in brains using qPCR. Sample RNAs were extracted from brains of mock-infected and TBEV-infected surviving and dying mice at 13 dpi (n = 4). The mRNA expression levels in TBEV-infected brains were normalized by GAPDH expression and are shown as the relative expression levels compared with mock-infected brains. Vertical error bars indicate the standard deviation of three independent experiments.

each mouse. T cells associated with surviving mice may also be variable and were divided into two groups based on CDR3 sequence patterns for VA8-1 and VB8-2. Thus, specific mechanisms to overcome TBEV infection may exist. It is therefore further worthwhile to investigate the roles of the distinct clones identified in our study, especially clones with VA15-1/AJ12, VB8-2/BJ2.1 (10 aa), and VA8-1/AJ15, that exhibited different patterns between surviving and dying mice.

The large sequence variation observed in our data can be explained by multiple reasons. First, TCR-peptide MHC (pMHC) recognition is flexible (1), and different TCRs with similar binding capabilities can recognize identical antigen peptides. Such flexibility may therefore produce variations in induced T-cell clones in TBEV-infected brains. Another possible reason relates to the presence of quasispecies. Noncloned RNA viruses generally exist as a quasispecies (22,25), and it has been reported that the virus stock used in our study was a complex of quasispecies (19). Consequently, the different amino acids for the antigen peptides among the quasispecies might produce T-cell clone variations in TBEV-infected brains.

We must also consider why different characteristics between surviving and dying mice were observed despite of an absence of differences between these groups in TCR repertoire analysis. Common V gene usage means that the TCR could recognize identical or similar antigen peptides (12,33). However, as described above, TCR-pMHC recognition can allow for some cross-reactivity; for example, different TCRs can bind to the same pMHC, and a single TCR can bind to a different pMHC (29,46). Therefore, TBEV infection can induce multiple T-cell clones with certain V genes that recognize specific antigens, yet only a few may play a critical role.

Different roles may also exist for the distinct T-cell clonotypes found in surviving and dying mice. However, qPCR analysis failed to identify any difference in T-cell function-associated markers between these groups, and apoptosis-associated genes were almost equivalently expressed in both surviving and dying mice. As this was the result for total brain expression, further studies of each T-cell clonotype are needed. We also need to investigate if the difference in target antigens recognized by T cells has an impact on severity and fatality rather than activation level. Or perhaps the difference in T-cell clonotype resulted from encephalitis progression and requires further investigation.

We must exercise care, because virulent and host immune responses can be very different in experimental models, depending upon the subtype and strain of virus, the mouse strain, and so on. In addition, because our data are based on analysis at 13 dpi only, we may need to investigate immune responses at earlier time points post-infection. We previously reported increased levels of serum corticosterone in dying mice (21). Glucocorticoids are known to exert immunomodulatory effects by activating the hypothalamic-pituitary-adrenal axis and/or cytokine expression (2,31). Thus, the relationship between T-cell clone bias and the level of corticosterone is interesting and warrants further investigation.

In conclusion, we have revealed an association between brain-infiltrating T-cell clones and severity in TBEV-infected mice, although the cause of this relationship is still unclear. Specifically, as the brain is originally free from adaptive immunity, it is unknown whether particular T-cell accumulation determines disease severity, or if a certain type of disorder induces particular T-cell accumulation by changing antigen presentation patterns. Further experiments are needed to elucidate which factor causes the difference in induced T-cell clones. Although our results are complicated, we believe our data are an initial step in better understanding of the mechanisms of viral encephalitis.

Acknowledgments

We thank the Tokyo Metropolitan Institute for Neuroscience for their assistance with animal experiments in the BSL3 laboratory.

This work was supported in part by Grants-in-Aid for Research on Emerging and Re-emerging Infectious Diseases by the Ministry of Health, Labour, and Welfare, Japan (grant H20-shinkou-ippan-015), and Research on Publicly Essential Drug and Medical Devices from the Japan Health Sciences Foundation (grants KH53333 and KHC3332).

Author Disclosure Statement

No competing financial interests exist.

References

1. Armstrong KM, Piepenbrink KH, and Baker BM: Conformational changes and flexibility in T-cell receptor recognition of peptide-MHC complexes. Biochem J 2008;415: 183–196.
2. Bailey M, Engler H, Hunzeker J, and Sheridan JF: The hypothalamic-pituitary-adrenal axis and viral infection. Viral Immunol 2003;16:141–157.
3. Bendelac A, Rivera MN, Park SH, and Roark JH: Mouse CD1-specific NK1 T cells: development, specificity, and function. Annu Rev Immunol 1997;15:535–562.
4. Brien JD, Uhrlaub JL, and Nikolich-Zugich J: Protective capacity and epitope specificity of CD8(+) T cells responding to lethal West Nile virus infection. Eur J Immunol 2007; 37:1855–1863.
5. Brien JD, Uhrlaub JL, and Nikolich-Zugich J: West Nile virus-specific CD4 T cells exhibit direct antiviral cytokine secretion and cytotoxicity and are sufficient for antiviral protection. J Immunol 2008;181:8568–8575.
6. Chiba N, Iwasaki T, Mizutani T, Kariwa H, Kurata T, and Takashima I: Pathogenicity of tick-borne encephalitis virus isolated in Hokkaido, Japan in mouse model. Vaccine 1999; 17:779–787.
7. Ding YH, Smith KJ, Garboczi DN, Utz U, Biddison WE, and Wiley DC: Two human T cell receptors bind in a similar diagonal mode to the HLA-A2/Tax peptide complex using different TCR amino acids. Immunity 1998;8: 403–411.
8. Dumpis U, Crook D, and Oksi J: Tick-borne encephalitis. Clin Infect Dis 1999;28:882–890.
9. Ecker M, Allison SL, Meixner T, and Heinz FX: Sequence analysis and genetic classification of tick-borne encephalitis viruses from Europe and Asia. J Gen Virol 1999;80(Pt1):179–185.
10. Fujii Y, Kitaura K, Nakamichi K, Takasaki T, Suzuki R, and Kurane I: Accumulation of T-cells with selected T-cell re-

ceptors in the brains of Japanese encephalitis virus-infected mice. Jpn J Infect Dis 2008;61:40–48.
11. Garboczi DN, Ghosh P, Utz U, Fan QR, Biddison WE, and Wiley DC: Structure of the complex between human T-cell receptor, viral peptide and HLA-A2. Nature 1996;384:134–141.
12. Garcia KC, and Adams EJ: How the T cell receptor sees antigen—a structural view. Cell 2005;122:333–336.
13. Garcia KC, Degano M, Pease LR, Huang M, Peterson PA, Teyton L, and Wilson IA: Structural basis of plasticity in T cell receptor recognition of a self peptide-MHC antigen. Science 1998;279:1166–1172.
14. Garcia KC, Degano M, Stanfield RL, *et al.*: An alphabeta T cell receptor structure at 2.5 A and its orientation in the TCR-MHC complex. Science 1996;274:209–219.
15. Glass WG, Lim JK, Cholera R, Pletnev AG, Gao JL, and Murphy PM: Chemokine receptor CCR5 promotes leukocyte trafficking to the brain and survival in West Nile virus infection. J Exp Med 2005;202:1087–1098.
16. Gritsun TS, Lashkevich VA, and Gould EA: Tick-borne encephalitis. Antiviral Res 2003;57:129–146.
17. Gritsun TS, Nuttall PA, and Gould EA: Tick-borne flaviviruses. Adv Virus Res 2003;61:317–371.
18. Hayasaka D, Goto A, Yoshii K, Mizutani T, Kariwa H, and Takashima I: Evaluation of European tick-borne encephalitis virus vaccine against recent Siberian and far-eastern subtype strains. Vaccine 2001;19:4774–4779.
19. Hayasaka D, Gritsun TS, Yoshii K, *et al.*: Amino acid changes responsible for attenuation of virus neurovirulence in an infectious cDNA clone of the Oshima strain of tick-borne encephalitis virus. J Gen Virol 2004;85:1007–1018.
20. Hayasaka D, Ivanov L, Leonova GN, *et al.*: Distribution and characterization of tick-borne encephalitis viruses from Siberia and far-eastern Asia. J Gen Virol 2001;82:1319–1328.
21. Hayasaka D, Nagata N, Fujii Y, *et al.*: Mortality following peripheral infection with tick-borne encephalitis virus results from a combination of central nervous system pathology, systemic inflammatory and stress responses. Virology 2009;390:139–150.
22. Holland JJ, De La Torre JC, and Steinhauer DA: RNA virus populations as quasispecies. Curr Top Microbiol Immunol 1992;176:1–20.
23. Horiuchi T, Hirokawa M, Kawabata Y, A. *et al.*: Identification of the T cell clones expanding within both CD8(+)CD28(+) and CD8(+)CD28(-) T cell subsets in recipients of allogeneic hematopoietic cell grafts and its implication in post-transplant skewing of T cell receptor repertoire. Bone Marrow Transplant 2001;27:731–739.
24. King NJ, Getts DR, Getts MT, Rana S, Shrestha B, and Kesson AM: Immunopathology of flavivirus infections. Immunol Cell Biol 2007;85:33–42.
25. Lauring AS, and Andino R: Quasispecies theory and the behavior of RNA viruses. PLoS Pathog 2010;6:e1001005.
26. Licon Luna RM, Lee E, Mullbacher A, Blanden RV, Langman R, and Lobigs M: Lack of both Fas ligand and perforin protects from flavivirus-mediated encephalitis in mice. J Virol 2002;76:3202–3211.
27. Lindquist L, and Vapalahti Q: Tick-borne encephalitis. Lancet 2008;371:1861–1871.
28. Lowenthal JW, Zubler RH, Nabholz M, and MacDonald HR: Similarities between interleukin-2 receptor number and affinity on activated B and T lymphocytes. Nature 1985;315:669–672.
29. Mason D: A very high level of crossreactivity is an essential feature of the T-cell receptor. Immunol Today 1998;19:395–404.
30. Matsutani T, Yoshioka T, Tsuruta Y, Iwagami S, and Suzuki R: Analysis of TCRAV and TCRBV repertoires in healthy individuals by microplate hybridization assay. Hum Immunol 1997;56:57–69.
31. Pinto RA, Arredondo SM, Bono MR, Gaggero AA, and Diaz PV: T helper 1/T helper 2 cytokine imbalance in respiratory syncytial virus infection is associated with increased endogenous plasma cortisol. Pediatrics 2006;117:e878–e886.
32. Purtha WE, Myers N, Mitaksov V, *et al.*: Antigen-specific cytotoxic T lymphocytes protect against lethal West Nile virus encephalitis. Eur J Immunol 2007;37:1845–1854.
33. Rudolph MG, Stanfield RL, and Wilson IA: How TCRs bind MHCs, peptides, and coreceptors. Annu Rev Immunol 2006;24:419–466.
34. Ruzek D, Salat J, Palus M, *et al.*: CD8+ T-cells mediate immunopathology in tick-borne encephalitis. Virology 2009;384:1–6.
35. Samuel MA, and Diamond MS: Pathogenesis of West Nile Virus infection: a balance between virulence, innate and adaptive immunity, and viral evasion. J Virol 2006;80:9349–9360.
36. Shrestha B, and Diamond MS: Fas ligand interactions contribute to CD8+ T-cell-mediated control of West Nile virus infection in the central nervous system. J Virol 2007;81:11749–11757.
37. Shrestha B, Samuel MA, and Diamond MS: CD8+ T cells require perforin to clear West Nile virus from infected neurons. J Virol 2006;80:119–129.
38. Takashima I, Morita K, Chiba M, *et al.*: A case of tick-borne encephalitis in Japan and isolation of the virus. J Clin Microbiol 1997;35:1943–1947.
39. Takeda T, Ito T, Chiba M, Takahashi K, Niioka T, and Takashima I: Isolation of tick-borne encephalitis virus from *Ixodes ovatus* (Acari: Ixodidae) in Japan. J Med Entomol 1998;35:227–231.
40. Takeda T, Ito T, Osada M, Takahashi K, and Takashima I: Isolation of tick-borne encephalitis virus from wild rodents and a seroepizootiologic survey in Hokkaido, Japan. Am J Trop Med Hyg 1999;60:287–291.
41. Tsuruta Y, Iwagami S, Furue S, Teraoka H, Yoshida T, Sakata T, and Suzuki R: Detection of human T cell receptor cDNAs (alpha, beta, gamma and delta) by ligation of a universal adaptor to variable region. J Immunol Methods 1993;161:7–21.
42. Vince V, and Grcevic N: Development of morphological changes in experimental tick-borne meningoencephalitis induced in white mice by different virus doses. J Neurol Sci 1969;9:109–130.
43. Wang F, Ono T, Kalergis AM, Zhang W, DiLorenzo TP, Lim K, and Nathenson SG: On defining the rules for interactions between the T cell receptor and its ligand: a critical role for a specific amino acid residue of the T cell receptor beta chain. Proc Natl Acad Sci USA 1998;95:5217–5222.
44. Wang Y, Lobigs M, Lee E, Koskinen A, and Mullbacher A: CD8(+) T cell-mediated immune responses in West Nile virus (Sarafend strain) encephalitis are independent of gamma interferon. J Gen Virol 2006;87:3599–3609.
45. Wang Y, Lobigs M, Lee E, and Mullbacher A: CD8+ T cells mediate recovery and immunopathology in West Nile virus encephalitis. J Virol 2003;77:13323–13334.

46. Wucherpfennig KW: T cell receptor crossreactivity as a general property of T cell recognition. Mol Immunol 2004;40:1009–1017.
47. Yokoyama WM, Koning F, Kehn PJ, Pereira GM, Stingl G, Coligan JE, and Shevach EM: Characterization of a cell surface-expressed disulfide-linked dimer involved in murine T cell activation. J Immunol 1988;141:369–376.
48. Yoshida R, Yoshioka T, Yamane S, Matsutani T, Toyosaki-Maeda T, Tsuruta Y, and Suzuki R: A new method for quantitative analysis of the mouse T-cell receptor V region repertoires: comparison of repertoires among strains. Immunogenetics 2000;52:35–45.

Address correspondence to:
Dr. Ryuji Suzuki
Department of Rheumatology and Clinical Immunology
Clinical Research Center for Allergy and Rheumatology
Sagamihara National Hospital
National Hospital Organization
18-1 Sakuradai, Minami-ku
Sagamihara, Kanagawa 252-0392, Japan

E-mail: r-suzuki@sagamihara-hosp.gr.jp

Received March 4, 2011; accepted April 2, 2011.

ORIGINAL ARTICLE

Prevalence of *Salmonella*, *Yersinia* and *Campylobacter* spp. in Feral Raccoons (*Procyon lotor*) and Masked Palm Civets (*Paguma larvata*) in Japan

K. Lee[1], T. Iwata[1], A. Nakadai[1], T. Kato[2], S. Hayama[2], T. Taniguchi[1] and H. Hayashidani[1]

[1] Division of Animal Life Science, Institute of Agriculture, Tokyo University of Agriculture and Technology, Tokyo, Japan
[2] Laboratory of Wildlife Medicine, Nippon Veterinary and Life Science University, Tokyo, Japan

Impacts

- This is the first report on the prevalence of *Salmonella*, *Yersinia*, and *Campylobacter* spp. in feral raccoons and masked palm civets in Japan.
- Our results indicate that these animals are potential carriers of these pathogens and that these animals probably acquired their infections from human activities, other wild animals, and the environment.
- As these animals live near human habitations or livestock farms, their carrying the pathogens represents a serious public and animal health risk.

Keywords:
Alien species; epidemiology; *Salmonella*; *Yersinia pseudotuberculosis; Campylobacter*

Correspondence:
H. Hayashidani. Division of Animal Life Science, Institute of Agriculture, Tokyo University of Agriculture and Technology, 3-5-8 Saiwai-cho, Fuchu, Tokyo 183-8509, Japan.
Tel.: +81 42 367 5775; Fax: +81 42 367 5775;
E-mail: eisei@cc.tuat.ac.jp

Received for publication September 28, 2009

doi: 10.1111/j.1863-2378.2010.01384.x

Summary

To estimate the public and animal health risk that alien species pose, the prevalence of *Salmonella*, *Yersinia*, and *Campylobacter* spp. in feral raccoons (*Procyon lotor*, $n = 459$) and masked palm civets (*Paguma larvata*, $n = 153$), which are abundant alien species in Japan, was investigated in urban and suburban areas of Japan. *Salmonella enterica* was detected from 29 samples [26 raccoons, 5.7%, 95% confidence interval (CI) 7.8–3.5%; three masked palm civets, 2.0%, 95% CI 4.2–0%]. Many of the isolates belonged to serovars that are commonly isolated from human gastroenteritis patients (e.g. *S.* Infantis, *S.* Typhimurium, and *S.* Thompson). The antimicrobial susceptibility test showed that 26.9 % of the isolates from raccoons were resistant to at least one antimicrobial agent, whereas none of the isolates from masked palm civets were resistant. *Yersinia* sp. was detected from 193 samples (177 raccoons, 38.6%, 95% CI 43.0–34.1%; 16 masked palm civets, 10.5%, 95% CI 15.3–5.6%). All virulent *Yersinia* strains belonged to *Yersinia pseudotuberculosis*, which was isolated from seven (1.5%, 95% CI 2.6–0.4%) raccoons and six (3.9%, 95% CI 7.0–0.8%) masked palm civets. According to the detection of virulence factors, all the *Y. pseudotuberculosis* isolates belonged to the Far Eastern systemic pathogenicity type. *Campylobacter* spp. was detected from 17 samples (six raccoons, 1.3%, 95% CI 2.3–0.3%; 11 masked palm civets, 7.2%, 95% CI 11.3–3.1%). Among these, three isolates from raccoons were identified as *C. jejuni*. These results showed that these pathogens can be transmitted by human activities, other wild animals, and the environment to feral raccoons and masked palm civets, and vice versa. As these animals have omnivorous behaviour and a wide range of habitats, they can play an important role in the transmission of the enteric pathogens.

Introduction

The raccoon (*Procyon lotor*) is a medium-sized mammal that is widely distributed in North America. Raccoons were introduced into Japan in the 1970s and have become naturalized in at least 42 of 47 prefectures (Ikeda et al., 2004). In urban areas, raccoons often use human houses for their dens. Raccoons use the feed stores of domestic animals as nests, and thus also have close contact with such animals (Zeveloff, 2002). It has been reported that the raccoon is a reservoir of various kinds of zoonotic pathogens in its place of origin, including the raccoon

roundworm (*Baylisascaris procyonis*) (Gavin et al., 2005), rabies virus (Finnegan et al., 2002), *Leptospira* spp. (Hamir et al., 2001), and *Francisella tularensis* (Berrada et al., 2006). Bigler et al. (1975) found that raccoons are so adaptive that they can bridge the gaps among avian, terrestrial, and aquatic environments, and thus they are appropriate as an indicator of the prevalence of various infectious diseases and pollutants. The masked palm civet (*Paguma larvata*) is also a medium-sized carnivore and is distributed widely in Asia. Masked palm civets are thought to have been introduced into Japan, although this contention is controversial (Abe, 2005). Masked palm civets often live in similar places as raccoons and can be carriers of human and animal pathogens, such as severe acute respiratory syndrome (SARS) virus (Tu et al., 2004) and canine distemper virus (Machida et al., 1992).

In Japan, attention has been focused on the role of these highly adaptive mammals in the transmission of zoonotic pathogens, including *Trichinella* T9 (Kobayashi et al., 2007), *Babesia microti*-like parasite (Kawabuchi et al., 2005), *Ehrlichia* spp., *Anaplasma phagocytophilum* (Inokuma et al., 2007), *Strongyloides procyonis* (Sato and Suzuki, 2006), and canine distemper virus (Machida et al., 1992). Pathogens carried by these animals can present serious public and animal health problems in the habitats to which they have been introduced. However, in spite of the fact that these two species often inhabit urban and suburban areas, there have been few reports on the prevalence of enteric pathogens among them.

The objective of this study was to determine the prevalence of the causal agents of enteric diseases including *Salmonella* spp., *Yersinia* spp., and *Campylobacter* spp. in feral raccoons and masked palm civets. We then assessed antimicrobial resistance in the isolates and analysed them using polymerase chain reaction (PCR) to elucidate their virulence factors and transmission routes.

Materials and Methods

Sample collection and transport

From March 2006 to May 2007, 459 feral raccoons and 153 feral masked palm civets were captured in Kanagawa, Gunma, and Tokyo Prefectures by each municipality as a part of the local governmental control and eradication programmes. The animals were caught using box traps and were killed by humanitarian methods (Japan Veterinay Medical Association, 2007). Of 459 feral raccoons, 229 (49.9%) were males, 211 (46.0%) were females, and 19 (4.2%) were of unknown sex. Of 153 feral masked palm civets, 72 (47.1%) were males, 79 (51.6%) were females, and two (1.3%) were of unknown sex. The age of the feral raccoons and masked palm civets was determined on the basis of tooth eruption and cranial suture obliteration by the method of Montgomery (1964) and Junge and Hoffmeister (1980). Of 459 feral raccoons, 71 (15.5%) were juveniles (<5 months), 357 (77.8%) were sub-adults or adults, and 31 (6.9%) were of unknown age. Of 153 feral masked palm civets, 47 (30.7%) were juveniles (<6 months), 104 (68.0%) were sub-adults or adults, and 2 (1.3%) were of unknown age. Faecal samples were collected and preserved in Cary and Blair transport medium (Eiken Chemical Co. Ltd., Tokyo, Japan) or sterile centrifuge tubes. The samples were then transported to the laboratory. The samples were suspended in 4 ml of sterile phosphate-buffered saline (PBS; pH 7.2) and tested within a week after collection.

Isolation and identification of *Salmonella*

One millilitre of each specimen was inoculated into 10 ml of buffered peptone water (BPW; Becton Dickinson, Franklin Lakes, NJ, USA). After incubation at 37°C for 24 h, 1 ml of BPW culture was transferred to 10 ml of Hajna-tetrathionate broth (Eiken Chemical). The broth was incubated at 37°C for 24 h, then one loopful of each tube was inoculated onto a plate of desoxycholate hydrogen sulfide lactose agar (DHL; Nissui Pharmaceutical Co. Ltd., Tokyo, Japan) and mannitol lysine crystal violet brilliant green agar (MLCB; Nissui). These plates were incubated at 37°C for 24 h, and at least two suspicious colonies morphologically similar to *Salmonella* spp. from each plate were subcultured for biochemical examinations. Biochemical characteristics were examined on triple sugar iron medium (Nissui) and lysine indole motility medium (Nissui). The subspecies of *Salmonella* isolates were confirmed by biochemical examinations and the multiplex PCR assay (Popoff and Le Minor, 2005; Lee et al., 2009). Serotyping for *Salmonella* isolates was accomplished with commercial O and H antisera (Denka Seiken Co. Ltd., Tokyo, Japan) according to the method of Popoff and Le Minor (2001).

Isolation and identification of *Yersinia*

Specimens were incubated at 4°C for 4 weeks. After alkali treatment (Aulisio et al., 1980), a loopful of sample suspension was spread on virulent *Yersinia enterocolitica* (VYE) agar (Fukushima, 1987) and Irgasan-Novobiocin (IN) agar containing 2.5 mg/l of irgasan and novobiocin in Yersinia Selective Agar Base (Difco Laboratories, Detroit, MI, USA) (Schiemann, 1979). All plates were incubated at 25°C for 48 h. Colonies morphologically similar to *Yersinia* spp. were subcultured for biochemical examination. The identification of yersiniae was performed by the methods of Wauters et al. (1988). All isolates identified as yersiniae were subjected to autoagglutination tests to evaluate their potential pathogenicity (Laird and Cavanaugh, 1980).

Then, virulent isolates were subjected to further analysis. Serotyping of *Y. pseudotuberculosis* was accomplished by slide agglutination with commercial antisera (Denka Seiken). Isolates identified as *Y. pseudotuberculosis* were genotyped by the presence patterns of the gene encoding *Y. pseudotuberculosis*-derived mitogen typeA (YPMa) and high-pathogenicity island (HPI) so as to analyse their geographical origin using PCR assay (Fukushima et al., 2001).

Isolation and identification of *Campylobacter*

One millilitre of the specimen was inoculated into 5 ml of Preston enrichment broth (OXOID CM0067 + SR0117E + SR0232E) containing 5% defibrinated horse blood. After incubation at 37°C for 24 h, one loopful of each tube was inoculated onto a skirrow blood agar plate (OXOID CM0271 + SR0069E + SR0232E) containing 5% defibrinated horse blood. All skirrow blood agar plates were incubated for 48 h at 37°C under microaerobic conditions and examined for the presence of characteristic colonies of *Campylobacter*. Confirmation and characterization of the isolates were performed on the basis of microscopic morphology, an oxidase test, a catalase test, growth at 25°C and 42°C, and a multiplex PCR assay for *C. jejuni*, *C. coli*, *C. lari*, *C. upsaliensis*, and *C. fetus* (Wang et al., 2002; Vandamme et al., 2005)

Antimicrobial susceptibility test

Antimicrobial susceptibility testing was performed according to the disc diffusion method (National Committee for Clinical Laboratory Standards, 2002; Luangtongkum et al., 2007). The following antimicrobial paper discs (Sensi-Disc; Becton Dickinson) were used: ampicillin (10 μg/disk), cefazolin (30 μg/disk), ceftriaxone (30 μg/disk), ciprofloxacin (5 μg/disk), chloramphenicol (30 μg/disk), gentamicin (10 μg/disk), kanamycin (30μg/disk), nalidixic acid (30 μg/disk), oxytetracycline (30 μg/disk), and streptomycin (10 μg/disk) for *Salmonella* and *Y. pseudotuberculosis*; and ampicillin, ciprofloxacin, clindamycin (2 μg/disk), erythromycin (15 μg/disk), gentamicin, kanamycin, nalidixic acid, norfloxacin (10 μg/disk), oxytetracycline, and streptomycin for *Campylobacter*.

Statistical analysis

Differences of the prevalence were analysed by the chi-squared test in SPSS software (SPSS Inc., Chicago, IL, USA).

Results

The raccoons and masked palm civets were essentially normal except for various external parasites. No discernible pathological evidence or signs of disease were observed. There were no significant sex- and age-specific differences in *Salmonella* spp., *Yersinia* spp., and *Campylobacter* spp prevalence in both animals (Table 1). There was no sample which was positive for more than two bacterial species or serotypes tested in this study, except non-pathogenic *Yersinia* spp.

Table 1. Prevalence of *Salmonella enterica*, *Yersinia pseudotuberculosis*, and *Campylobacter* sp. in raccoon and masked palm civets in each sex or age groups

			No. positive sample (%)		
Origin	Sex/age	Sample size	*Salmonella enterica*	*Y. pseudotubeculosis*	*Campylobacter* spp.
Raccoon	Female	211	11 (5.2)	2 (0.9)	2 (0.9)
	Male	229	15 (6.6)	5 (2.2)	3 (1.3)
	Unknown	19	0	0	1 (5.3)
	Juvenile	71	2 (2.8)	1 (1.4)	0
	Sub-, Adult	357	24 (6.7)	6 (1.7)	5 (1.4)
	Unknown	31	0	0	1 (3.2)
	Total	459	26 (5.7)	7 (1.5)	6 (1.3)
Masked palm civet	Female	79	1 (1.3)	3 (3.8)	7 (8.9)
	Male	72	2 (2.8)	3 (4.2)	4 (5.6)
	Unknown	2	0	0	0
	Juvenile	47	1 (2.1)	3 (6.4)	5 (10.6)
	Sub-, Adult	104	2 (1.9)	3 (2.9)	6 (5.8)
	Unknown	2	0	0	0
	Total	153	3 (2.0)	6 (3.9)	11 (7.2)

